NATIONAL ADVISORY COMMITTEE FOR AERONAUTICS

TECHNICAL NOTE 1920

PRELIMINARY INVESTIGATION OF NEEDLE BEARINGS OF $1\frac{1}{8}$-INCH PITCH DIAMETER AT SPEEDS TO 17,000 rpm

By E. Fred Macks

Lewis Flight Propulsion Laboratory
Cleveland, Ohio

Washington
August 1949

NATIONAL ADVISORY COMMITTEE FOR AERONAUTICS

TECHNICAL NOTE 1920

PRELIMINARY INVESTIGATION OF NEEDLE BEARINGS OF $1\frac{1}{8}$-INCH PITCH DIAMETER AT SPEEDS TO 17,000 rpm

By E. Fred Macks

SUMMARY

An analysis of the factors involved in the high-speed operation of needle bearings including stresses due to maneuvering loads, deformations due to operation at high temperatures, and internal forces within the bearing is presented. An expression for end thrust was derived wherein end thrust was found to be approximately equal to the external load multiplied by an over-all equivalent coefficient of friction. This equivalent coefficient of friction was experimentally obtained over a wide range of operating conditions.

An experimental investigation of $1\frac{1}{8}$-inch-pitch-diameter needle bearings over a range of shaft speeds between 2000 and 17,000 rpm, loads from 3.5 to 600 pounds per square inch (based on bearing projected area; that is, product of pitch diameter and effective needle length), and oil flows from 0.5 to 24 pounds per hour emphasized that the operating characteristics of needle bearings are largely dependent upon speed, external load, needle length-diameter ratio, and needle diameter. With length-diameter ratios of 3.50 and 2.75, operation at shaft-pitch-surface speeds up to 80 feet per second was possible. Operation of needle bearings with a needle length-diameter ratio of 5.71 or greater was unsatisfactory at shaft-pitch-surface speeds in excess of 30 to 40 feet per second. The length-diameter ratio was unreliable as the main criterion upon which to base needle-bearing performance inasmuch as bearings with length-diameter ratios of 11.67 operated better than bearings with length-diameter ratios of 5.71, these bearings having essentially the same length needles. Therefore with shaft deflection present, the stiffness of the needle was a significant factor.

The experimental results for the end thrust developed within a needle bearing agreed qualitatively with the derived expression. The over-all equivalent coefficient of friction for all the bearings investigated decreased with increase in speed from a value of 0.07 at 2000 rpm to a value of 0.04 at 13,000 rpm.

In general, the percentage of slip within the bearings increased with increase in speed. The data indicated that at low loads the orbital needle speed may become independent of shaft speed at high values of shaft speed. The percentage of slip decreased with increase in load at a given speed. The inner (rotating) race was far more vulnerable than the outer (stationary) race with regard to scuffing, wear, and chatter marks and should therefore be given every consideration regarding lubrication, surface finish, tolerances, and mounting accuracy.

From the results of this preliminary investigation, needle bearings are not recommended for high-speed applications where appreciable shaft deflections may be present.

INTRODUCTION

A high-speed long-life bearing to carry radial load, to have low breakaway torque, and preferably to operate at high temperatures is desired for use as the turbine-support bearing in gas-turbine-type aircraft-propulsion units as well as for other high-speed applications. Conventional rolling-contact bearings present cage, cooling, and lubrication problems at extreme speeds. One of the main disadvantages of the sleeve bearing is its high breakaway torque, which is significant at low temperatures.

Several papers (references 1 to 6), published during 1930-36, describe the construction, principle of operation, and application of the needle bearing. The mechanism of operation of this bearing has been considered by some investigators (references 1 and 4) to be different from that of any other type bearing. Unit sliding of the needles as a full-floating sleeve is believed to occur under ordinary operating conditions — the individual needles rolling about their own axes only under conditions of overload and severe shock. This theory has also been advanced as explanation of the higher load-carrying capacity of the needle bearing as compared with the conventional roller bearing, the assumption being made that load is carried not only by the needles along their lines of contact but also by the lubricant in the wedge-shaped spaces between the needles (reference 4). Many investigators who do not agree with the foregoing theory of needle motion claim that all the needles have a continuous rolling action about their respective axes (for example, reference 5). Another investigator (reference 7) has reported that during operation the needles of a properly designed needle bearing rotate only in the region beneath the load and then in a predictable pattern, whereas the needles of an improperly designed bearing continuously rotate.

The investigation reported herein was conducted at the NACA Lewis laboratory to determine experimentally the operating characteristics of needle bearings. Analyses of the factors involved in the high-speed operation of needle bearings and a description of the apparatus employed to investigate the operating characteristics at high speeds are included.

The investigation was conducted on bearings of $1\frac{1}{8}$-inch pitch diameter with needle length-diameter ratios of 2.75 to 11.67 and various diametral clearances at maximum unit loads up to 600 pounds per square inch (based on bearing projected area), oil flows up to 24 pounds per hour, and shaft speeds up to 17,000 rpm.

ANALYSIS

Stresses and Deformation

Under ordinary flight conditions, the rotor-support bearings of gas-turbine units support only the weight of the rotating assembly in the radial direction and the algebraic sum of the individual axial forces developed by the turbine and the compressor. During flight maneuvers, however, inertial and gyroscopic forces are set up in the radial direction, and inertial axial forces (due to aircraft acceleration) are imposed in the axial direction, all of which must be accommodated by the rotor-support bearings. The gyroscopic reaction couple may be appreciable for a swiftly spinning body whose straight-line path of motion is abruptly altered. In addition to these external loads, a load that is equal to the product of the needle mass and the centripetal acceleration and that acts upon the needle and the outer race is set up within the bearing during operation.

Stresses. - Stribeck (reference 8) correlated Hertz's theory (reference 9) with his own empirical data and thereby originated the equations, which, with certain refinements (reference 10), are currently used to determine the unit stresses within rolling-contact bearings. The stress for a turbine-support bearing from a typical turbine during normal operating conditions as calculated using the aforementioned formula and under a gravity load of 357 pounds is approximately 69,000 pounds per square inch. The maximum short-duration stress encountered during severe maneuvers, such as aircraft spin, is approximately 282,000 pounds per square inch as calculated using a value of the angular velocity of 3 radians per second. Consequently, although the gravitational load is relatively small, the unit stresses within the bearing may become quite high.

When the effective length of the rolling element is less than the race width, the ends of the contact area have a higher unit load than does the rest of the area inasmuch as work is done in compressing race material laterally as well as in the direction of rolling (reference 11). This edge stress may be as much as one and one-half times the calculated value of the mean stress for the area of contact (the mean stress being approximately 0.8 of the maximum stress for line contact). This edge pressure has been relieved in many roller-bearing designs by crowning the rollers or the races; however, such a practice is not generally followed by needle-bearing manufacturers.

Deformations. - Neither Hertz nor Stribeck obtained the deflection relations for cylindrical bodies. However, formulas have been developed by several other investigators (references 11 to 14).

In order to determine the effect of temperature on deformation, Palmgren's expressions (reference 12) for deflection in a cylindrical roller bearing may be combined to give

$$\delta = K' \left(\frac{1}{E}\right)^{0.9} \qquad (1)$$

(All symbols used throughout this report are defined in the appendix.)

The modulus of elasticity of steel is

$$E = 30.5 \times 10^6 - 1.5 \times 10^4 \, T$$

The calculated ratio of the deflection at a surface temperature of 400° F to the deflection at 25° F is 1.2. Therefore, when radial deflections are significant, the effect of temperature upon deflection should be considered.

Internal Forces

The internal forces that act upon a needle bearing may be grouped as follows:

(1) Centrifugal forces
(2) Separating forces
(3) Axially developed forces
(4) Radially developed forces due to skewing

Centrifugal forces. - The centrifugal force per needle F_c is calculated according to Newton's second law. The value of centripetal acceleration, which is dependent on the orbital needle speed (the rotative speed of the needle body about the shaft center), is

$$a = \frac{D_p}{2}\left(\frac{2\pi N'_n}{60}\right)^2, \tag{2}$$

and, for the case of no slippage,

$$N'_n = \frac{1}{2} N_s \left(1 - \frac{D}{D_p}\right) \tag{3}$$

Newton's second law may be combined with equations (2) and (3) to give

$$F_c = 0.7881\times10^{-6}\, D^2 \rho N_s^2\, D_p \left[\left(1 - \frac{D}{D_p}\right)^2\right] \tag{4}$$

Equation (4) has been plotted for various needle-bearing dimensions and shaft speeds in figure 1.

Centrifugal force tends to throw the rolling elements of a rolling-contact bearing radially outward, and at high speeds and light external loads the centrifugal load thus created may significantly influence operating characteristics of the bearing.

Separating forces. - The separating forces may be defined as those forces that act on the moving elements at the pitch diameter and in a direction tangential thereto. The subject of separating forces within rolling-contact bearings has received little attention in the literature, presumably because the magnitudes involved are small; however, the presence of separating forces influences the operation of a needle-type bearing.

The separating forces in a needle bearing are caused by:

(1) Shaft eccentricity of inner race with respect to outer race
(2) Needle drag
(3) Angular acceleration of rotating race

Shaft eccentricity results from internal radial clearance C and deflection δ of the needles and races due to load P (figs. 2(a) and 2(b)). A third source that causes a cyclic change

in the separating force during normal operation is the shaft rise and fall δ_r (fig. 2(c)) due to rotation of the needles beneath the load and thereby a change in the load-deflection curve between two adjacent load-carrying elements; this phenomenon is described for ball bearings by Perret (reference 10).

The separating forces are indicated in figure 3(a). Line contact (at a maximum surface speed of twice the shaft-surface speed) occurs between adjacent needles. Even when the separating forces are small, there is little possibility of an oil film building up between adjacent needles inasmuch as the relative motion of their surfaces at the line of contact is in a direction opposite to that necessary to produce a hydrodynamic film, and wear of the needles is therefore an inevitable outcome (fig. 3(b)).

The needle drag increases with an increase in oil flow and with an increase in speed and generally decreases with an increase in bearing temperature. This drag opposes the separating forces due to shaft eccentricity in the region 180° before the load and augments them in the region 180° after the load.

Angular acceleration of the rotating race causes inertial drag forces within the needle circle; this additional drag may cause appreciable sliding and subsequent wear of the rolling elements, especially during high accelerations.

Axially developed forces. - If present, taper of the rolling elements causes one end to move farther than the other end in a given time and thereby causes skewing. Shaft deflection or taper of the races also tends to produce skewing. Factors such as asymmetry of lubricant or friction distribution and centrifugal force acting upon the rolling elements and upon the lubricant may also pivot the rolling element within the clearance space. Whenever skewing occurs, sliding takes place and results in the generation of a larger amount of heat within the bearing than would occur if pure rolling occurred.

The approximate stress distribution and the position of a representative needle in the loaded zone for a shaft with and without deflection are shown in figure 4. The bearing is assumed to be precisely manufactured in that no taper or other irregularity exists within the bearing; it is also assumed that the outer race is rigidly mounted. Without shaft deflection the needles ride as shown in figure 4(a), whereas with shaft deflection and zero shaft speed the needles ride either as shown in figures 4(b) or 4(c).

Based on the assumptions that the needles are located as shown in figure 4(b), that at the beginning of shaft rotation the needle axes are parallel with the outer race, and that no skewing exists, the approximate load distribution between a representative needle and the inner race and the forces due to race friction will be as shown in figures 4(b) and 5(a), respectively. In these figures, the inner race and the needle make contact in the region of point A, which is closer to one end of the needle than to the other end. In order to prevent skewing, the summation of moments about a vertical axis through point A must equal zero, thus

$$F_o'(z-b) - \bar{F}_o b = 0 \tag{5}$$

Neglecting centrifugal force on the rolling element, lubricant churning, and deflection at the zones of contact in equation (5) gives

$$W\frac{b}{z}\bar{\mu}_r(z-b) - W\left(\frac{z-b}{z}\right)\bar{\mu}_r b = 0 \tag{6}$$

Equation (6) is true only if the average coefficient of rolling friction is the same on either side of point A. However, if centrifugal force on the rolling element and lubricant churning are considered, the moments about point A will be such as to cause skewing of the rolling element.

During operation in a skewed position, the needle tip will be loaded against the outer-race flange. Inasmuch as this needle-tip load affects the net axial load on the outer race, an expression relating the variables entering into the development of the needle-tip load is derived. If a representative needle in the loaded zone rides as shown in figure 5(c), the forces acting will then be as shown. For the needle to remain in equilibrium, the summation of moments about a vertical axis through point A must equal zero; therefore

$$W'(z-b)\sin\alpha+\bar{W}b\sin\beta+F_o'(z-b) + G_n\mu_s\left[\frac{l}{2} - \left(b-\frac{z}{2}\right)\right] + zK_i V_{n,i}\left(b-\frac{z}{2}\right)$$

$$= \bar{F}_o b+G_n\left[\frac{l}{2} - \left(b-\frac{z}{2}\right)\right]\tan\phi+zK_o V_{n,o}\left(b-\frac{z}{2}\right) \tag{7}$$

where

$$W' = \frac{Wb\cos\theta\cos\phi}{z} + \frac{G_n D}{2(z-b)} + \frac{F_c}{2}$$

$$\overline{W} = W\left(\frac{z-b}{z}\right) \cos\theta \cos\phi + \frac{F_c}{2}$$

$$F_o' = W'(\mu_s \sin\phi + \mu_r \cos\phi)$$

$$\overline{F}_o = \overline{W}(\mu_s \sin\phi + \mu_r \cos\phi)$$

$$\alpha = \frac{(z-b)(\phi)}{R}$$

$$\beta = \frac{b\phi}{R}$$

Substituting these values into equation (7), solving for G_n, and simplifying give

$$G_n = \frac{K-2W\left[\frac{b}{z}(z-b)\cos\phi(\sin\alpha\cos\theta+\sin\beta\cos\theta)\right] - F_c(z-b)\cos\phi(\sin\alpha+\mu_s\sin\phi+\mu_r\cos\phi)}{l(\mu_s\cos\phi-\sin\phi)-2\left(b-\frac{z}{2}\right)\cos\phi(\mu_s-\tan\phi)+D(\sin\alpha+\mu_s\sin\phi+\mu_r\cos\phi)} -$$

$$\frac{-F_c\, b\cos\phi(\sin\beta-\mu_s\sin\phi-\mu_r\cos\phi)}{l(\mu_s\cos\phi-\sin\phi)-2\left(b-\frac{z}{2}\right)\cos\phi(\mu_s-\tan\phi)+D(\sin\alpha+\mu_s\sin\phi+\mu_r\cos\phi)} \qquad (8)$$

where

$$K = 2z\left(b-\frac{z}{2}\right)\cos\phi\,(K_o V_{n,o} - K_i V_{n,i})$$

Substituting the following approximate orders of magnitudes in equation (8) gives

$$G_n \cong 10K-0.1W-0.1F_c \tag{9}$$

where

b	is of order of 0.5
z	1.0
μ_s	.1
μ_r	.0001
sin α	.01
cos α	1.0
sin β	.01
cos β	1.0
sin θ	.001
cos θ	1.0
sin $\phi \cong$ tan ϕ	.01
cos ϕ	1.0
D	.1
l	1.0
$\left(b-\frac{z}{2}\right)$	.1
(z-b)	.5

That the angle of skew appreciably affects the magnitude of G_n may be seen when sin ϕ of the order 0.1 instead of 0.01 is substituted in equation (8) (corresponding values of sin α and sin β change from 0.01 to 0.1); thus

$$G_n \cong 100K-10W-10F_c \tag{10}$$

If sin ϕ is of the order 0.001 instead of 0.01 and the values of α and β are also of the order 0.001, the following expression results:

$$G_n \cong 10K-0.01W-0.01F_c \tag{11}$$

Asymmetrical churning forces may appreciably affect G_n. Also, when churning forces are neglected, the value of G_n is quite small for small angles of skew, even under appreciable loads.

The approximate maximum values of the angles involved in equation (8) for a given bearing may be calculated (neglecting needle deflection and assuming $\alpha = \beta$) from the expressions

$$\alpha \cong \cos^{-1}\left(1-\frac{C}{R}\right) \tag{12}$$

and

$$\phi \cong \frac{2R\alpha}{z} \tag{13}$$

or ϕ may be limited by the circumferential clearance rather than the radial clearance, in which case

$$\phi \cong \cos^{-1}\left(\frac{D}{D+c}\right) \tag{14}$$

The smallest value obtained from either equation (13) or (14) is the maximum possible skewing angle. For bearings with relatively large diametral clearances, the maximum possible angle of skew is generally given by equation (14). Also, the required unbalanced couple becomes greater as ϕ is increased. It is therefore probable that under moderate and heavy external loads ϕ, α, and β will be small. This point is further discussed in the section, Discussion of Experimental Results.

Equation (8) contains terms for which values are not known with sufficient accuracy to make the equation quantitatively useful. However, this equation is qualitatively useful in that it shows how each variable contributes to the needle-tip load G_n. For example, inasmuch as the needle moves opposite to the direction of rotation relative to the rotating race and moves in the direction of rotation relative to the stationary race, the lubricant churning forces will affect the needle pivoting moment in relation to the radial distribution of the lubricant between the inner and outer races. That is, if the radial distribution of lubricant is uniform, the churning moments will be balanced; however, if the lubricant is more plentiful in the vicinity of the outer race, the needle will tend to pivot

about point A in a counterclockwise direction and conversely if the lubricant is more abundant in the vicinity of the inner race (fig. 5(b)). As shaft speed increases, two additional factors occur simultaneously: both roller and lubricant have a greater orbital speed about the shaft center thereby giving rise to higher centrifugal forces. If the centrifugal force acting on the needle is assumed to act at its center of gravity, equation (6) will no longer be true because F_o' and $\overline{F}_o$ will increase in like amounts, but inasmuch as $\overline{F}_o$ has a greater effective moment arm, the needle will tend to pivot in a counterclockwise direction (fig. 5(b)). The resisting churning motion, however, is also in a counterclockwise direction because the lubricant is more abundant at the outer race. These effects are vectorially additive, and the tendency to skew may be increased or decreased by an increase in speed depending upon the original angle of skew.

A factor that affects application of the foregoing conclusions at high speed and relatively light loads is slippage between the needles and the inner race and consequent decrease in orbital needle speed. As needle slippage increases, the relative motion between the needles and the rotating race increases whereas that between the needles and the stationary race decreases, thus causing a net churning moment of the needle in a clockwise direction (fig. 5(b)).

The evaluation of these forces during skewing becomes more complicated because of shaft deflection, or taper of the bearing elements, when the zones of contact between the needle and the inner and outer races are asymmetrical, permitting leakage between the needles and the races in the circumferential direction. This leakage effects a change in the churning forces, which in turn alters the skewing moments. Inasmuch as it has been observed that more slippage occurs as the speed increases (for a given load) and that speed and churning have opposite effects upon needle skewing, the problem of evaluating the net result of these effects over a wide operating range is difficult.

The end thrust per needle acting on the outer race is found as follows: With skewing present, the needle has axial components of velocity in opposite directions relative to the inner and outer races. With equal loads and coefficients of friction at the inner and outer races, the friction forces resulting from the foregoing relative velocities will balance and there will be no net axial force on the needle. However, with unequal loading and churning, the needle-tip force is introduced. The end thrust G' acting on the outer race due to a single needle in the loaded zone (figs. 5(c) and 5(d)) is

$$G' = G_{W'} + G_{\overline{W}} + G_n \tag{15}$$

where

$G_{W'} = W'(\mu_s \cos \phi - \mu_r \sin \phi)$

$G_{\overline{W}} = \overline{W}(\mu_s \cos \phi - \mu_r \sin \phi)$

Substituting the preceding quantities in equation (15) gives

$$G' = (W' + \overline{W})(\mu_s \cos \phi - \mu_r \sin \phi) + G_n \tag{16}$$

Because ϕ and μ_r are small, equation (16) reduces to

$$G' = (W' + \overline{W})\mu_s + G_n \tag{17}$$

Inasmuch as W', $\overline{W}$, and μ_s are generally unknown, equation (17) may be rewritten in terms of the actual load W and an equivalent coefficient of friction μ' as

$$G' = \mu' W + G_n \tag{18}$$

In order to evaluate equation (18), the angles ϕ, α, and β and the asymmetrical churning forces or representative average values of these variables must be known. These representative average values are obtained by empirical methods and therefore equation (18) is discussed in the section, Discussion of Experimental Results. Allan (reference 15) obtained an expression for end thrust (neglecting several of the aforementioned variables) equal to the product of load multiplied by the coefficient of combined rolling and sliding friction. Allan's expression is essentially that of equation (18) if the needle-tip load is negligible compared with $\mu' W$.

The condition of needle skewing may be internally improved by needle-end guidance, by crowning of the needles or races, by controlling the diametral and circumferential clearance, or by more precise manufacturing tolerances of needles and races. The amount of skew may be externally improved by keeping shaft deflection to a minimum or by providing the bearing with a self-alining outer housing.

Radially developed forces. - The unit load acting at the inner race is increased because of skewing (that is, reduction in area of contact), whereas the unit load at the outer race is increased

because of both skewing and centrifugal force (fig. 5). At the outer race, the increase in unit load may be attributed to the reduction in area of contact, to the centrifugal force, and to the effective components of the load, which are greater than the load itself, at the contact points. The unbalanced churning forces also affect the radial loads at the contact zones.

Internal motion. - It is desirable to know the exact motions within a needle bearing inasmuch as these motions affect the operating characteristics to a marked degree. Some investigators (references 11 and 12) believe that in a conventional roller bearing the rollers are in intimate contact with the races at all times and therefore rotate about their centers at a speed dependent on the ratio of the inner-race diameter to the roller diameter, and that the rollers rotate about the shaft center with an orbital speed N'_n according to equation (3). However, isolated cases have been found in the literature, as in reference 16, where at high speeds and under light radial load, cage speed was found to be independent of shaft speed. In such a case considerable slip occurs within the bearing, the internal load developed within the bearing is less than that theoretically predicted, and under such operating conditions, some hydrodynamic action rather than intimate rolling contact possibly exists, thereby reducing the fatigue problem for high-speed lightly loaded roller bearings. Rolling action of the rollers at all times, even in roller bearings, is undesirable because of the fatigue phenomena involved. If a bearing could be evolved that would inherently demonstrate rolling action upon starting and stopping (thereby giving low wear and low breakaway torque) and oil-film sliding under normal operating conditions, longer bearing life would result. However, sliding must occur over an oil film if flat spots on the rollers are to be prevented.

APPARATUS AND PROCEDURE

Apparatus. - All the bearings investigated had a pitch diameter of approximately $1\frac{1}{8}$ inches. The location of the experimental bearing was such that one end was unobstructed for observation of the component parts during operation. The needle motion was observed through a glass end plate under illumination from a stroboscopic light source (fig. 6).

Because of the anticipated application of the results of this investigation to aircraft gas-turbine units for which low loads prevail and appreciable deflection and misalinement is possible, the

experimental shaft was so designed that it would impose approximately 0.001 inch of shaft deflection per inch of bearing length at the experimental bearing under a load of 350 pounds on the experimental bearing (fig. 7). (This value of deflection is the maximum recommended by needle-bearing manufacturers.) This entire deflection may be ineffective at the experimental bearing inasmuch as the outer race of the bearing is mounted in a housing that is floated on a high-pressure oil film (described later) and that may be partly self-alining. The load was applied to the shaft through a nonsupported bearing by a lever and static weights. One-half of the applied load was taken by the experimental bearing and the other half by a support ball bearing at the drive end of the shaft.

The shaft assembly used in the investigation is shown in figure 8. Lubricating oil under pressure was introduced to the experimental bearing through a rotating pressure joint. The support bearings were splash-lubricated by an adjustable, sight oil feeder, which directed oil on a dummy gear mounted on the shaft between the load and the support bearings.

The measurement of friction torque and end thrust was accomplished by a free-floating externally pressurized bearing housing (fig. 9) and dynamometer rings equipped with resistance-wire strain gages in a Wheatstone bridge circuit (reference 17). A spring ball-and-groove-type linkage was incorporated in the friction-torque arm. The force necessary to pull this linkage apart was less than that necessary to cause permanent deflection in the dynamometer ring. Both friction torque and end thrust were recorded by means of a photoelectric potentiometer recorder with an accuracy of ±3 percent.

The motion of the rolling elements was studied through a glass end plate by means of a stroboscopic light source for most of the runs. A disadvantage of this method was that at some operating conditions the orbital needle speed was nonuniform and the average value could not be determined; also, for certain values of oil flow and shaft speed, the needles could not be clearly seen because of oil bubbles between the needle ends and the glass end plate. A telescope with a photosensitive element in place of the usual objective lens was built and mounted in front of the bearing so that a light beam falling on the cell from a source behind the bearing was broken as each needle passed by, the impulses being amplified and read by an oscilloscope (fig. 10). A system of an air-cooled mercury arc lamp with a lens to focus the intense beam of light on a mirror that in turn directed the parallel beam through colinear slots in the bearing end plate was unsuccessful because of oil bubbles within the bearing. Later in the investigation, a battery-energized pickup coil (fig. 11) was incorporated in the externally

pressurized housing. As each needle passed beneath the pole piece of the winding, the lines of flux were disturbed and the impulse thus generated was amplified and detected by a frequency meter. In this manner, an average as well as an instantaneous value of orbital needle speed was available. This method worked well during the runs for which it was employed.

A speed increaser was coupled to a 3-horsepower variable-speed unit on one end and to the experimental shaft on the other by a shear-pin coupling and a flexible coupling, respectively. The speed range of the shaft was from 2000 to 17,000 rpm; shaft speed was measured by a chronometric tachometer.

A temperature-regulating valve automatically blended warm and cool oil in the proper proportions to give a preset value of oil temperature. The oil pressure to the experimental bearing was controlled by means of a regulator, which was also used to control the flow of oil to this bearing; the pressure was read to ±0.1 pound per square inch. The flow was measured to within ±0.005 pound per hour by two rotameters of different range in parallel. High-pressure oil (1200 lb/sq in.) was supplied to float the experimental-bearing housing. Oil from the entire unit drained by gravity to a sump wherein a float actuated the pump switch in such a manner that only solid oil was returned to the oil reservoir.

Temperatures were read by means of a self-balancing potentiometer and copper-constantan thermocouples to within ±0.5° F. The temperature within the experimental unit was measured as was the oil entering the experimental shaft. The needle-bearing temperature was obtained by a thermocouple held against the loaded side of the outer race by a set screw at the axial center line. The load-bearing and support-bearing temperatures were obtained by spring-loaded thermocouples pressed against the outer races.

Experimental bearings. - The bearings investigated were made to the same pitch diameters for the following reasons: Friction torque rather than coefficient of friction is used to compare the results, and it is at the pitch diameter that the average friction torque acts. The internal loading in very high-speed rolling-contact bearings, which is in part due to the centrifugal force of the rolling elements, affects the life of the bearings. Because this internal load is dependent upon the pitch diameter for rolling-contact bearings, eliminating this variable is advantageous when comparing the operating characteristics of various types of bearing at high speeds. Also, the value of pitch diameter is more indicative of the average size of the various bearing types than is the shaft diameter.

Hampp, in testing cylindrical roller bearings at pitch-surface speeds up to 29 feet per second (reference 18), found that increase in diametral clearance reduced end thrust, friction torque, and bearing temperature; therefore, the experimental bearings used in the investigation were designed with relatively large diametral clearances, that is, ranging from about 0.001 to 0.003 inch.

A copper-lead sleeve bearing was used for the break-in runs of the apparatus (fig. 12 and table I). The inner races of the sleeve bearing and of the needle bearings were 3/4 inch long with a 1/8-inch radial oil hole at the axial midpoint. Inasmuch as a new inner and outer race were required for each run, these components were designed to be a thumb-push fit on the shaft and in the housing. The inner race was rigidly clamped against a shoulder on the shaft. Except for the run that employed the magnetic pickup, no special effort was made to keep the outer race from slowly rotating; this condition is believed desirable in order to eliminate local wear on the normally stationary race of a unidirectionally loaded bearing. In spite of early difficulty encountered with fretting corrosion at the load- and support-bearing bores, no difficulty was caused by fretting corrosion of the experimental journal under almost identical mounting conditions (0.0001 to 0.0002 in. loose shaft to bearing-bore fits).

Physical characteristics of the bearings investigated are given in table I. The needles for the needle bearings were purchased in lots of 500, the manufacturers' tolerances being 0.0002 inch in diameter and 0.020 inch in length. The needles were measured by an electrolimit gage set with gage blocks and sorted into groups with a tolerance of 0.00005 inch in diameter and ±0.005 inch in length. The needles have spherical ends with a radius equal to the diameter of the needle. The effective needle length is taken as the over-all length minus the spherical overhang at each end. The race diameters were measured and checked for concentricity and taper by an electrolimit gage set with gage blocks. Tolerances of 0.0002 inch for concentricity and total taper were maintained for the bearing races used. The designed circumferential spacing of the needles was 0.0001 inch per needle for each bearing investigated.

The hardness of the needle-bearing races was less than that recommended by some bearing manufacturers; this condition was the result of fabrication from SAE 4140, which will not harden beyond Rockwell C-57. Inasmuch as the bearings were used for relatively short runs, this deficiency should not invalidate comparison of the results obtained.

Procedure. - Oil having the properties given in figure 13 was used during the investigation.

The temperature of the oil as it entered the experimental shaft was held approximately constant between 85° and 92° F for all the investigations reported herein. It should be mentioned, however, that this oil passed through a hole in the shaft almost the length of the shaft before it was introduced to the bearing under investigation. Undoubtedly a temperature change, which varied with the oil flow and operating conditions, was thus incurred; the exact temperature of the oil as it entered the bearing is therefore unknown.

In order to determine the effect of speed upon the operating characteristics, load and oil flow were held constant for a given speed during the runs; after the experimental-bearing temperature had essentially reached equilibrium, the readings were taken and the load was then increased to the next predetermined value. In order to determine the effect of oil flow upon operating characteristics, speed and load were held constant for a given oil flow during a run; after equilibrium was essentially established, readings were taken and the oil flow was then increased to the next predetermined value.

The end thrust of some of the bearings investigated was erratic for certain conditions of operation. Inasmuch as there was considerable axial play (0.020 in.) in the end-thrust linkage so as to allow for zero checks of the strain-gage readings, a violent vibration was sometimes set up and the reading fluctuated considerably. An average reading was taken in such cases.

The orbital needle speed was determined by a stroboscopic light source whenever the readings were not obscured by oil bubbles or by random motion. The percentage of slip is defined as

$$\text{percentage of slip} = \left(\frac{N'_n - N_n}{N'_n}\right) 100$$

The starting or breakaway torque of the experimental bearing was first measured by a photoelectric potentiometer recorder that had a full-scale indicator response of 1/2 second. Comparison of the maximum-response slope with the slope of actual starting torque data indicated that the value of starting torque reached a maximum either at or before 1/2 second. Values of starting torque measured in this manner may therefore be less than the true values. The

breakaway torque was subsequently determined as that torque required just to begin bearing rotation when a tangential force was gradually applied to the bearing housing through a spring scale. An average of ten readings was made to determine an accepted value for a given load.

RESULTS AND DISCUSSION

Experimental Results

The results of the runs on bearings are given in table I and in figures 12 and 14 to 29. (Compressive end thrust means that the end-thrust linkage to the dynamometer ring was in compression.) The load acting on the experimental bearing is given in pounds per square inch (based on the product of the effective needle length and the bearing pitch diameter). All the failures occurred on bearings that had an effective needle length-diameter ratio l/D of 5.71 or greater.

Influence of speed and load on operating characteristics. - The effects of speed and load upon the operating characteristics of the bearings investigated are given in figures 12 and 14 to 16 and the following general observations may be made therefrom:

(1) The operation was generally satisfactory (bearing equilibrium temperatures established) for light loads at shaft-pitch-surface speeds up to 80 feet per second if the needle l/D ratio was 3.50 or less. However, the operating characteristics were unsatisfactory (seizure occurred) for needle l/D ratios of 5.71 or greater — especially for shaft-pitch-surface speeds in excess of 30 to 40 feet per second.

(2) Bearings with l/D ratios of 11.67 operated better than bearings with l/D ratios of 5.71, these bearings having essentially the same length needles. Therefore with shaft deflection present, the stiffness of the needle is a significant factor.

(3) The end thrust developed within the bearing generally decreased with increase in speed. The end thrust increased approximately linearly with increase in load, the slope being somewhat different for each bearing investigated. The magnitude of end thrust was less for small values of needle l/D ratio than for large values of this ratio for a given unit bearing load.

(4) When large values of end thrust occur, the values of friction torque did not always increase with an increase in load or in bearing operating temperature; in some cases the friction torque decreased with an increase in load or in bearing temperature.

(5) The failed bearings all showed scoring of the inner race and of the needles; no evidence of failure was indicated by visual inspection of the outer race (fig. 16).

Influence of oil flow on operating characteristics. - The effect of oil flow on the operating characteristics is shown in figures 17 to 20. The general observations that may be made are:

(1) For a given operating condition there exists a flow rate above which or below which bearing operating temperature decreases. For a given bearing, this critical flow rate is dependent upon the operating condition but generally decreases as load increases at a given speed.

(2) In many cases at very light loads, high speeds, and low oil flows, increase in oil flow up to a certain value of flow decreases the value of friction torque. Above this critical flow rate, the torque increases with increase in oil flow. At higher values of load the friction torque is generally proportional to the oil flow.

(3) For small values of end thrust, change in oil flow has little effect; however, when end thrust is appreciable, an increase in flow may cause a decrease in end thrust and may even reverse the direction.

(4) The supply pressure of oil fed to the bearing through the inner race must be increased at a rate greater than the rate of speed increase in order to maintain a constant flow of oil to the bearing (figs. 12, 14, and 15).

Breakaway torque. - The variation of breakaway torque with load, as determined by the spring-scale method, is shown for the sleeve bearing in figure 21; and the results for several needle bearings are given in figure 22.

For each of the needle bearings investigated, the breakaway torque was considerably greater when the needles were in a skewed position. Inasmuch as the average maximum value of starting torque is of interest, readings were made when the needles were in a skewed position; the average of ten readings was used for a given point.

The scatter shown is the deviation between maximum and minimum values of the ten readings that were averaged for each point. For loads above 100 pounds per square inch, the general observations evident from a comparison of figures 21 and 22 are as follows:

(1) The breakaway torque of the needle bearings investigated is much less than for a sleeve bearing of comparable size.

(2) The breakaway coefficient of friction for the bearings with skewed needles varied from 0.0075 to 0.056 over the range of loads investigated.

(3) The breakaway coefficient of friction without skewing of the needles, calculated from the data of figure 22, was as low as 0.0005.

Internal motion. - The results of the visual study of motion within four of the bearings are given in figure 23 in which the percentage of slip is shown as a function of shaft-pitch-surface speed. The data of needle bearing 3 have been replotted in figure 24 for comparison with data for a size 306 commercial roller bearing operating up to 36,000 rpm (reference 16), the ordinate scale being relative for the two bearings.

Inasmuch as it was impossible to determine the orbital needle speeds at high values of shaft speed by the visual method due to oil churning, the magnetic pickup was used to obtain readings at all values of shaft speed for needle bearing 4 (figs. 25 to 27). At low loads and for a given operating condition, the readings could be reproduced if the load was not removed or if the machine was not stopped between the readings. However, if the load was removed and then reapplied or the machine stopped and then brought up to apparently identical operating conditions, the amount of slip was generally nonreproducible. This fact may be observed in figure 25 and by comparing figures 25, 26, and 27. Inasmuch as the orientation of the needles within the bearing (as affected by removal and application of load and by starting and stopping) is so critical regarding the percentage of slip within the bearing, the results must be taken qualitatively rather than quantitatively.

The following general observations may be made:

(1) For a given load, and particularly at light loads, the percentage of slip increases with an increase in speed, the orbital needle speed possibly becoming independent of high values of shaft speed. (See figs. 23 and 24.)

(2) The percentage of slip decreases with an increase in load at a given speed.

(3) The percentage of slip is slightly affected by the oil flow to the bearing within the flow ranges investigated (fig. 27).

Discussion of Experimental Results

End thrust generally decreases with an increase in speed and increases approximately as a straight line with an increase in load, which indicates that operation may be occurring in the boundary region of lubrication (reference 19 wherein, at high values of surface speed, the coefficient of sliding friction μ_s is reported to decrease with increase in speed). However, the magnitude of this reduction in μ_s with speed is insufficient to account for the decrease in end thrust with speed observed in this investigation. It is well established that in the fluid-film region of operation, the coefficient of friction increases with an increase in speed if the other variables remain constant.

As mentioned in the ANALYSIS section, equation (18) cannot be quantitatively evaluated until average values of churning forces and angles ϕ, α, and β are at hand. The following approximate method may be used to estimate the order of magnitude of α, β, and ϕ:

If the needle-tip load and friction forces that have a straightening effect on a skewed needle are assumed negligible, if α is assumed equal to β, and if W' is assumed equal to $\overline{W}$ and to $W/2$, then the couple M' resisting skewing will be

$$M' \cong \frac{W}{2} z \sin \alpha \tag{19}$$

(It should be noted that the net effect of the foregoing assumptions in all probability tends to make M', and therefore ϕ, larger than exists in practice.)

The friction force per needle at the outer race may be estimated if the friction torque for the bearing is known for a given operating condition. Assuming that one-third of the needles (those in the loaded zone) contribute in a large part to the friction torque gives the resistance d_m to motion for these needles as

$$d_m \cong \frac{M}{(D_p/2)(n/3)} \tag{20}$$

In order to be on the extremely conservative side, that is, to make ϕ, α, and β as large as possible, this entire force is assumed to act at a moment arm $z/2$.

Therefore,

$$M' \cong \frac{3\ z\ M}{n\ D_p} \tag{21}$$

Setting equations (19) and (21) equal and making use of the fact that for the needle directly under the load $W = 5P/n$ (reference 8) give

$$\alpha \cong \sin^{-1}\left(\frac{M}{D_p\ P}\right) \tag{22}$$

Using the experimental data of needle bearing 4 (fig. 14(c)) as an example and substituting the following values

$$P = (600\ \text{lb/sq in.})\left(\frac{2.75}{8}\right)(1.116)(16) = 3680\ \text{oz}$$

$$M = 9.2\ \text{oz-in. (at } N_s \text{ of 2000 rpm)}$$

$$D_p = 1.116$$

$$l = 0.343$$

into equation (22) give

$$\alpha \cong \sin^{-1}\left[\frac{9.2}{(1.116)(3680)}\right] \cong \sin^{-1}(0.0025)$$

$$\alpha \cong \beta \cong 0^\circ\ 9'$$

thus, from equation (13)

$$\phi \cong 0^\circ\ 30'$$

However, from equation (12), needle bearing 4 has a possible value of α equal to

$$\alpha \cong \cos^{-1}\left(1 - \frac{\frac{0.0025}{2}}{\frac{1.116+0.1250}{2}}\right)$$

$$\alpha \cong \cos^{-1}(0.998)$$

$$\alpha \cong \beta \cong 3^\circ\ 30'$$

thus, from equation (13), $\phi \cong 13^\circ$. However, from equation (14),

$$\phi \cong \cos^{-1}\left(\frac{0.1250}{0.1250+0.0001}\right)$$

$$\phi \cong 2^\circ\ 20'$$

The maximum possible angle of skew is therefore defined by equation (14) rather than by equation (13). Also, the probable maximum operating angle is considerably less than the maximum possible value (that is, $0^\circ\ 30'$ compared with $2^\circ\ 20'$ in this case).

For smaller loads, the operating angles become larger (this statement applies to the needles in the more lightly loaded regions of a heavily loaded bearing as well as to the needles under the load in a lightly loaded bearing). As previously stated, in all probability the net effect of the assumptions contained in the foregoing analysis tends to make the angles larger than they would actually be. Equation (18) rewritten in terms of the total external load P and an over-all equivalent coefficient of friction μ'', which incorporates G_n in a psuedo fashion, gives the following expression for the resultant end thrust G" acting on the outer race

$$G'' = \mu''P \tag{23}$$

Thus, if the end thrust for a representative group of bearings can be measured over a wide operating range, the values of the over-all equivalent coefficient of friction μ'' may be determined and used in estimations of end thrust to be expected in design applications.

The values of end thrust for the needle bearings investigated are shown plotted against total load (fig. 28) for shaft speeds of 2000, 8000, and 13,000 rpm. The slope of the faired curve for each speed may be taken as the average value of the over-all equivalent coefficient of friction μ''. These average values of μ'' have been plotted against shaft speed in figure 29, wherein it is shown

that μ'' decreases with increase in speed. The manner in which the variables entering the problem affect the resultant end thrust has been discussed in the ANALYSIS section (equations (5) to (18)).

The effect of shaft deflection upon end thrust may be determined by inspection of the data of figure 28. As indicated in this figure for a given load and therefore a given shaft deflection, the bearings with large l/D ratios develop about the same end thrust as do the bearings with smaller l/D ratios. It is thus probable that the data obtained by the apparatus described herein are in a large part dependent upon the load-deflection curve of the experimental shaft (fig. 7). It is possible that this objectionable feature may be eliminated in future runs by investigating all bearings in a self-alining housing, which will be required in actual practice if needle bearings are to operate under the most favorable conditions.

The fact that, when large values of end thrust occur at very small values of friction torque, the friction torque does not always increase with an increase in load and in some cases actually decreases makes it doubtful that friction torque and end thrust as measured were completely independent of one another. Although this detail has been given every consideration, it is questionable that the two readings are entirely independent when the end thrust acts to compress the linkage connecting the floating housing and the dynamometer ring; the data presented herein should therefore be analyzed with this fact in mind.

Scoring of the inner race and of the needles of failed bearings indicated that the inner race takes a good deal more punishment during operation than does the outer race. This scoring may in part be attributed to the higher stresses imposed upon the inner race because of the smaller area of contact between the inner race and needles than between the outer race and needles. However, the loads employed were relatively light, and it is believed that the smaller area of contact at the inner race, together with skewing, and the fact that the lubricant is thrown outward tending to starve this zone are the primary causes of failure. Inasmuch as temperature of the bearing is a decisive criterion of its satisfactory operation, the foregoing statements make it evident that temperature should be measured at the inner race as well as at the outer race.

When the oil is supplied through a radial hole in the inner race of a needle bearing, the oil-feed pressure must be increased at a somewhat greater rate than the increase in shaft speed to maintain a constant supply of oil to the bearing (figs. 14 and 15).

That the percentage of slip cannot be reproduced in all cases for apparently the same operating conditions under light loads might be explained by change in needle orientation and lubricant distribution upon starting and stopping and upon the removal and the reapplication of load. It is likely that vibrations of the shaft and housing are also critical factors in determining slip within the bearing.

The effect of diametral clearance cannot be established from this preliminary investigation inasmuch as the data are inconclusive.

SUMMARY OF RESULTS

From the analysis and the experimental investigation of $1\frac{1}{8}$-inch-pitch-diameter needle bearings over a range of shaft speeds, loads per square inch of bearing projected area, and oil flows, the following results were obtained:

1. An expression for the end thrust was derived wherein the end thrust was found to be approximately equal to the total external load multiplied by an over-all equivalent coefficient of friction.

2. Operation of needle bearings with needle length-diameter ratios of 5.71 or greater was unsatisfactory for shaft-pitch-surface speeds in excess of 30 to 40 feet per second.

3. With length-diameter ratios of 3.50 and 2.75, operation up to 80 feet per second was possible.

4. The length-diameter ratio was unreliable as the main criterion upon which to base needle-bearing performance inasmuch as bearings with length-diameter ratios of 11.67 operated better than bearings with length-diameter ratios of 5.71, these bearings having essentially the same length needles. Therefore, with shaft deflection present, the stiffness of the needle was a significant factor.

5. The over-all equivalent coefficient of friction for all the bearings investigated remained essentially independent of external load and decreased with increase in speed.

6. In many cases at light loads, high speeds, and low oil flows, increase in oil flow up to a certain value of flow decreased the value of friction torque. Above this critical flow rate, the torque increased with increase in oil flow. At higher values of load, the friction torque was generally proportional to the oil flow.

7. If oil were fed through the inner race of a needle bearing, the feed pressure would have to be increased at a somewhat greater rate than the increase in shaft speed in order to maintain a constant oil flow through the bearing.

8. The breakaway torque of needle bearings, even with needle skewing present, was much less than for a copper-lead sleeve bearing of comparable size.

9. The over-all equivalent coefficient of friction for all the bearings investigated decreased with increase in speed from a value of 0.07 at 2000 rpm to a value of 0.04 at 13,000 rpm.

10. For a given load, the percentage of slip within the bearing increased with an increase in speed. The data indicated that at low loads the orbital needle speed may become independent of shaft speed at high values of shaft speed. The percentage of slip decreased with an increase in load at a given speed.

11. The inner race was much more vulnerable than the outer race with regard to scuffing, wear, and chatter marks and should therefore be given every consideration regarding lubrication, surface finish, tolerances, and mounting accuracy.

From the results of this preliminary investigation, needle bearings are not recommended for high-speed applications where appreciable shaft deflections may be present.

Lewis Flight Propulsion Laboratory,
National Advisory Committee for Aeronautics,
Cleveland, Ohio, May 6, 1949.

APPENDIX - SYMBOLS

The following symbols are used in this report:

a	centripetal acceleration, in./sec^2
b	longer distance along needle axis from center of contact zone of needle and inner race (point A) to center of contact zone of needle and outer race, in.
C	internal radial clearance of bearing, in.
$\overline{C}$	total diametral clearance, in.
c	circumferential clearance per needle, in.
D	needle diameter, in.
D_p	pitch diameter of bearing, in.
d_m	resistance to motion of all needles in loaded zone, lb
E	modulus of elasticity, lb/sq in.
F_c	centrifugal force per needle, lb
F_d	drag force when adjacent needle is not propelling itself at orbital speed, lb
F_i	friction force perpendicular to shaft axis acting between needle and inner race, lb
F_l	lubricant shear force, lb
F_m	motive force of more highly loaded needle, lb
F_o'	friction force perpendicular to shaft axis acting between needle and outer race over length (z-b), lb
$\overline{F}_o$	friction force perpendicular to shaft axis acting between needle and outer race over length b, lb
F_s	separating force due to shaft eccentricity acting at right angles to line from outer-race center to contact zone between inner race and needle, lb
f	breakaway coefficient of friction

G' end thrust acting on outer race due to single needle in loaded zone, lb

G'' resultant end thrust acting on outer race, lb

G_n needle-tip force due to skewing, lb

G_W axial force on inner race (or shaft) due to algebraic summation of $G_{W'}$, $G_{\overline{W}}$, G_n, and $W \sin \theta$ (that is, $G_W = G_{W'} + G_{\overline{W}} + G_n - W \sin \theta$), lb

$G_{W'}$ axial force on outer race due to W', lb

$G_{\overline{W}}$ axial force on outer race due to $\overline{W}$, lb

K $2z\left(b-\frac{z}{2}\right) \cos \phi \, (K_o V_{n,o} - K_i V_{n,i})$

K' constant

K_i churning factor per unit needle length per unit relative velocity of needle with respect to inner race

K_o churning factor per unit needle length per unit relative velocity of needle with respect to outer race

l needle length, in.

M friction torque, lb-in.

M' couple resisting skewing, lb-in.

N speed, rpm

N_n actual orbital needle speed, rpm

N'_n theoretical orbital needle speed, rpm

N_s shaft speed, rpm

n number of rolling elements per bearing

P external bearing load, lb

Q oil flow, lb/sec

R	inside radius of outer race, in.
r	outside radius of inner race, in.
T	temperature, ^{o}F
$V_{n,i}$	relative velocity of needle with respect to inner race
$V_{n,o}$	relative velocity of needle with respect to outer race
W	external load per needle, lb
W'	load acting between needle and outer race, which may be considered to be concentrated at distance (z-b) from point A, lb
$\overline{W}$	load acting between needle and outer race, which may be considered to be concentrated at distance b from point A, lb
z	distance between center of contact zones of needle and outer race along needle axis, in.
α	angle of skew of needle from point A to (z-b), end view, deg
β	angle of skew of needle from point A to b, end view, deg
δ	deflection, in.
δ_r	shaft rise and fall due to rotation of needles beneath load, in.
θ	angle that load makes with shaft axis (see fig. 4), deg
μ_r	coefficient of rolling friction
$\overline{\mu}_r$	average coefficient of rolling friction
μ_s	coefficient of sliding friction
μ''	over-all equivalent coefficient of friction
ϕ	angle of skew of needle, plan view, deg

REFERENCES

1. Pitner: Les roulements à aiguilles et leurs applications. Jour. de Soc. des Ing. l'Auto, 4 Ann., T. III, No. 6, Juin 1930, pp. 1051-1061.

2. Anon.: Needle Bearings Offer Advantages in High Speed Automotive Engines. Auto. Ind., vol. 63, no. 24, Dec. 13, 1930, pp. 869-870.

3. Brownback, Henry Lowe: Steel Needles May Solve High Speed Bearing Problem. Motorboat, vol. 27, no. 12, Dec. 1930, p. 19.

4. Ferretti, Pericle: Experiments with Needle Bearings. NACA TM 707, 1933.

5. Clark, Allen F.: Needle Bearings – Unique Machine Elements. Machine Design, vol. 5, no. 8, Aug. 1933, pp. 31-34, 43.

6. Anon.: The Needle-Roller Bearing. Engineering, vol. CXLI, April 10, 1936, pp. 392-393.

7. Paterson, E. V.: Needle Roller Bearings. The Auto. Eng., vol. XXXIV, no. 448, April 1944, pp. 147-150.

8. Stribeck: Ball Bearings for Various Loads. A.S.M.E. Trans., vol. 29, 1907, pp. 420-463; discussion, pp. 464-467.

9. Hertz, Heinrich: Gesammelte Werke, Bd. I. Johann Ambrosius Barth (Leipzig), 1895, pp. 155-173.

10. Perret: The Effect of Bearing Play on the Load Capacity of Antifriction Bearings. Trans. No. F-TS-595-RE, Air Materiel Command, Army Air Forces, Aug. 14, 1946.

11. Allan, R. K.: Roller Bearings. Isaac Putnam & Sons, Ltd. (London), 1945.

12. Palmgren, Arvid: Ball and Roller Bearing Engineering. S. H. Burbank & Co., Inc. (Philadelphia, Pa.), 1945.

13. Föpple, L.: Der Spannungszustand und die Anstrengung des Werkstoffes bei der Berührung zweier Körper. Forschung auf dem Gebiete des Ingenieurwesens, Ausg. A, Bd. 7, Nr. 5, Sept./Okt. 1936, pp. 209-221.

14. Timoshenko, S., and Baud, R. V.: The Strength of Gear Teeth. Mech. Eng., vol. 48, no. 11, Nov. 1926, pp. 1105-1109.

15. Allan, R.: End Thrust of Parallel Roller Bearings. Machinery (London), vol. 60, no. 1546, May 28, 1942, p. 494.

16. Wilhelm, W. F., Jr.: 36,000 rpm Tests of Hyatt BU 0306-Z Roller Bearings. Res. Rep. SR-320, Westinghouse Res. Labs., Westinghouse Elec. Corp., Nov. 27, 1945.

17. Shaw, Milton C., Strang, Charles D., and Hart, Ormal W.: Measurement of Piston-Ring Radial-Pressure Distribution. SAE Quarterly Trans., vol. 2, no. 1, Jan. 1948, pp. 169-189.

18. Hampp: Influence of Design Dimensions upon the Operational Performance of Roller-Bearings. Trans. No. F-TS-604-RE, Air Materiel Command, Army Air Forces, June 15, 1946.

19. Johnson, Robert L., Swikert, Max A., and Bisson, Edmond E.: Friction at High Sliding Velocities. NACA TN 1442, 1947.

TABLE I - PHYSICAL CHARACTERISTICS AND RESULTS OF RUNS ON BEARINGS INVESTIGATED

Bearing	Bearing type	Effective length-diameter ratio	Needle diameter (in.)	Bearing pitch diameter (in.)	Average diametral clearance (in.)	Number of needles	Race hardness, Rockwell C	Oil flow (lb/hr)	Maximum shaft speed (rpm)	Maximum shaft-pitch-surface speed (ft/sec)	Maximum load (lb)	Maximum unit load (lb/sq in.)	Remarks
1	Copper-lead sleeve	(a)	------	[b]1.118	0.0024	-----	[c]52-57	1.4 to 3.6	16,600	81.3	168	200	Used for comparative data
2	Commercial needle	2.75	0.137	1.137	0.0010	26	60-65	2	16,700	82.9	117	300	Satisfactory operation
3	Needle	2.75	0.1249	1.116	0.0018	28	52-57	2	16,700	81.4	117	300	Satisfactory operation
4	Needle	2.75	0.1249	1.116	0.0025	28	52-57	2	16,700	81.4	230	600	Satisfactory operation
5	Needle	5.71	0.1249	1.116	0.0018	28	52-57	2	8000	39.0	237	300	Failed at 12,000 rpm with 0 load as speed was increased from 8000 rpm
6	Needle	5.71	0.1248	1.116	0.0020	28	52-57	2	13,000	63.3	79	[d]100	Failed at 13,000 rpm with load of 136 lb/sq in. after running at 13,000 rpm with load of 100 lb/sq in.
7	Needle	3.50	0.0625	1.117	0.0016	56	52-57	0.5	16,700	81.4	147	600	Satisfactory operation
8	Needle	3.50	0.0625	1.117	0.0028	56	52-57	0.5	16,700	81.4	147	600	Satisfactory operation
9	Needle	11.67	0.0624	1.117	0.0017	56	52-57	2	13,000	63.3	243	[d]300	Failed at 16,000 rpm with 0 load as speed was increased from 2000 rpm; had run at 13,000 rpm with load of 300 lb/sq in.
10	Needle	11.67	0.0625	1.117	0.0027	56	52-57	12	16,600	81.4	81	100	Failed after running for 8 min at 16,600 rpm with load of 100 lb/sq in.

[a]Length-diameter ratio of 0.67 for over-all bearing.
[b]Bore.
[c]Shaft hardness.
[d]Maximum unit load at which bearing operated satisfactorily at indicated speed.

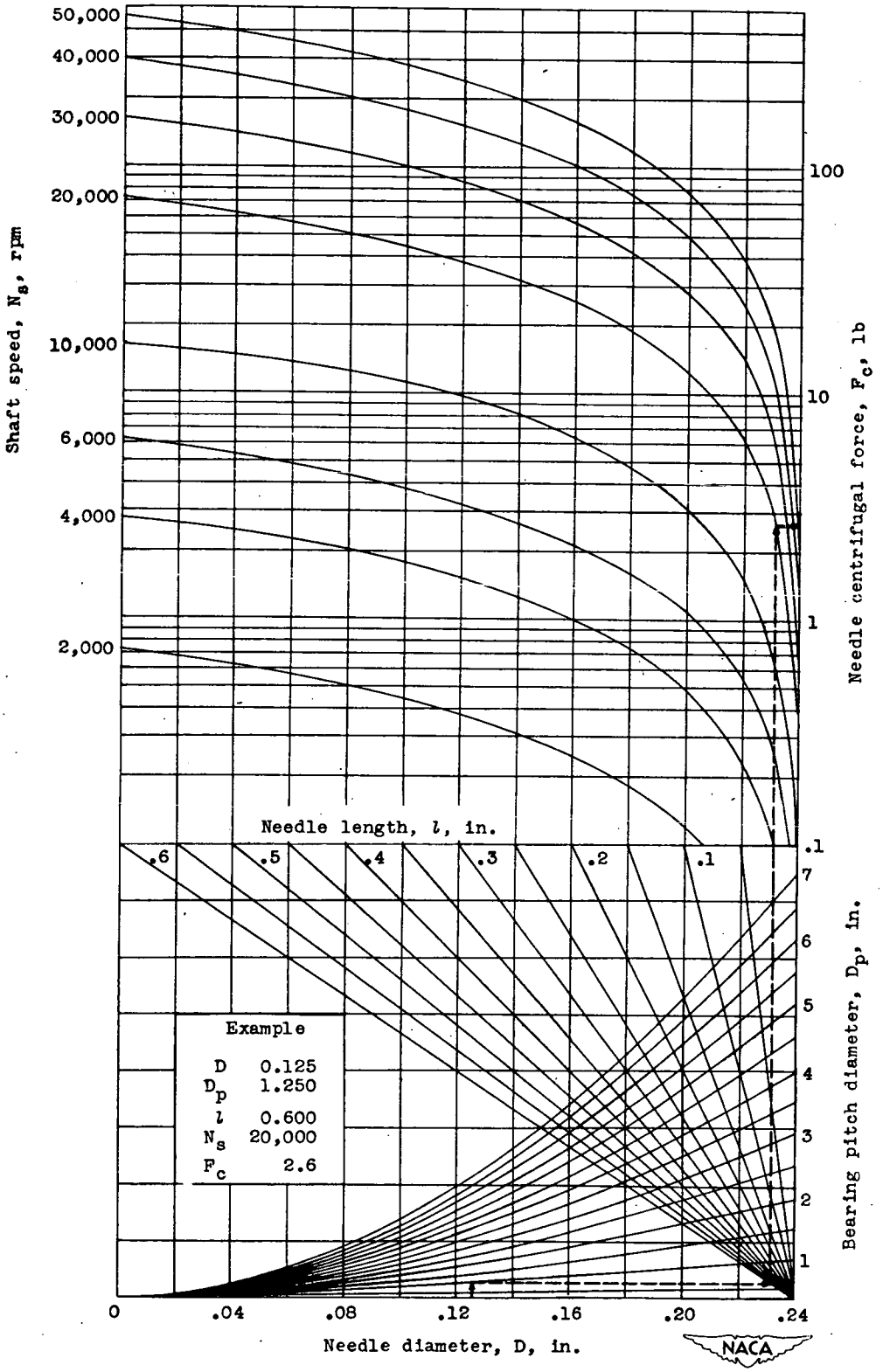

Figure 1. - Variation of needle centrifugal force with bearing dimensions and shaft speed (equation (4)).

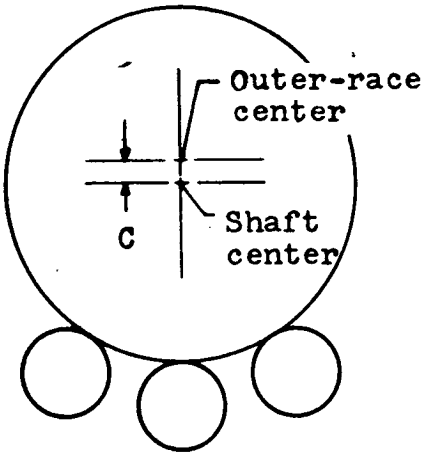

(a) No load, no rotation.

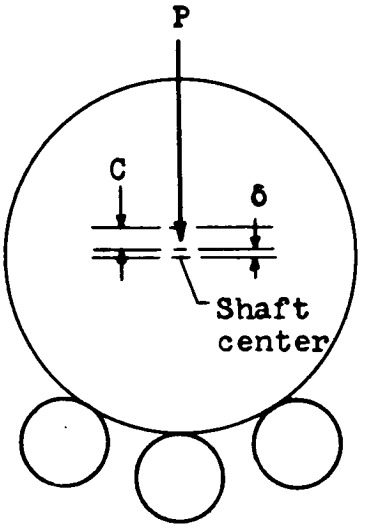

(b) Load, no rotation.

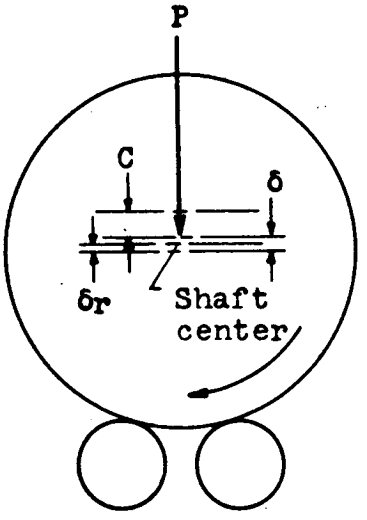

(c) Load and rotation.

Figure 2. - Variation of shaft-center location of rolling-contact bearing for conditions of no load and no rotation, load and no rotation, and load and rotation.

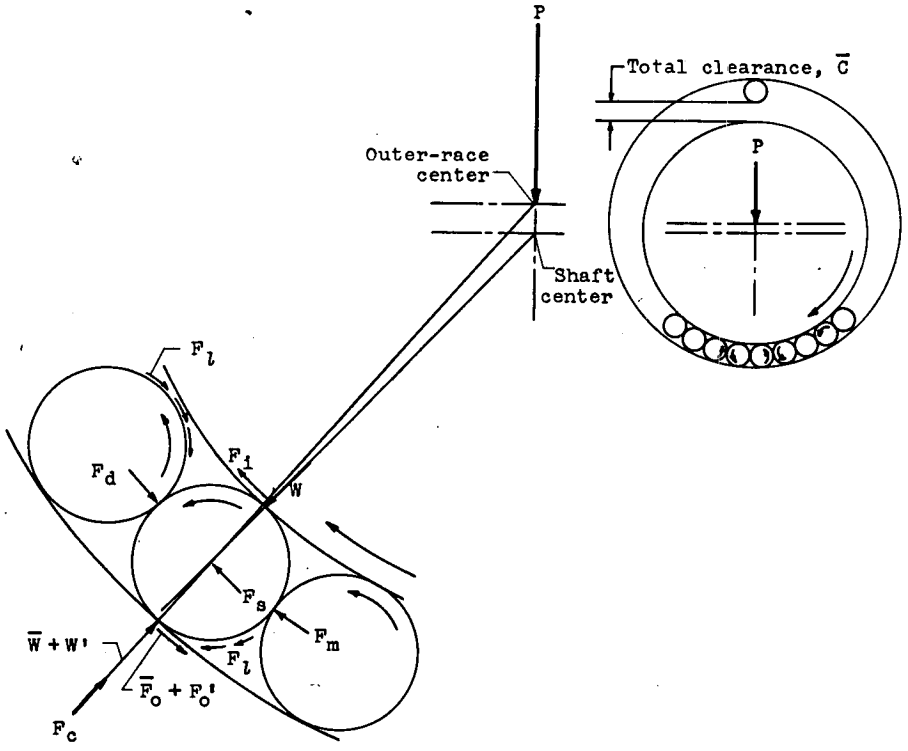

(a) Forces (friction forces between needles not shown).

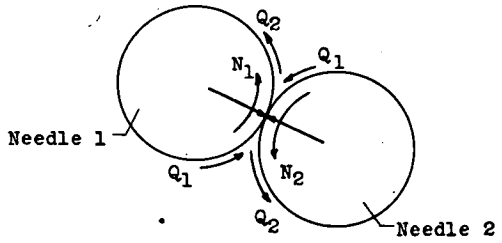

Q_1 quantity of oil carried between needles under load

Q_2 quantity of oil carried away from needles under load

If $N_1 \cong N_2$ then $Q_1 \cong Q_2$ (equivalent to zero oil flow between needles under load). Inasmuch as oil-film shear beneath load vector is absent, no positive oil-film pressure between needles can develop.

(b) Oil film between adjacent needles.

Figure 3. - Forces acting on rolling element of and the motion within a conventional needle bearing.

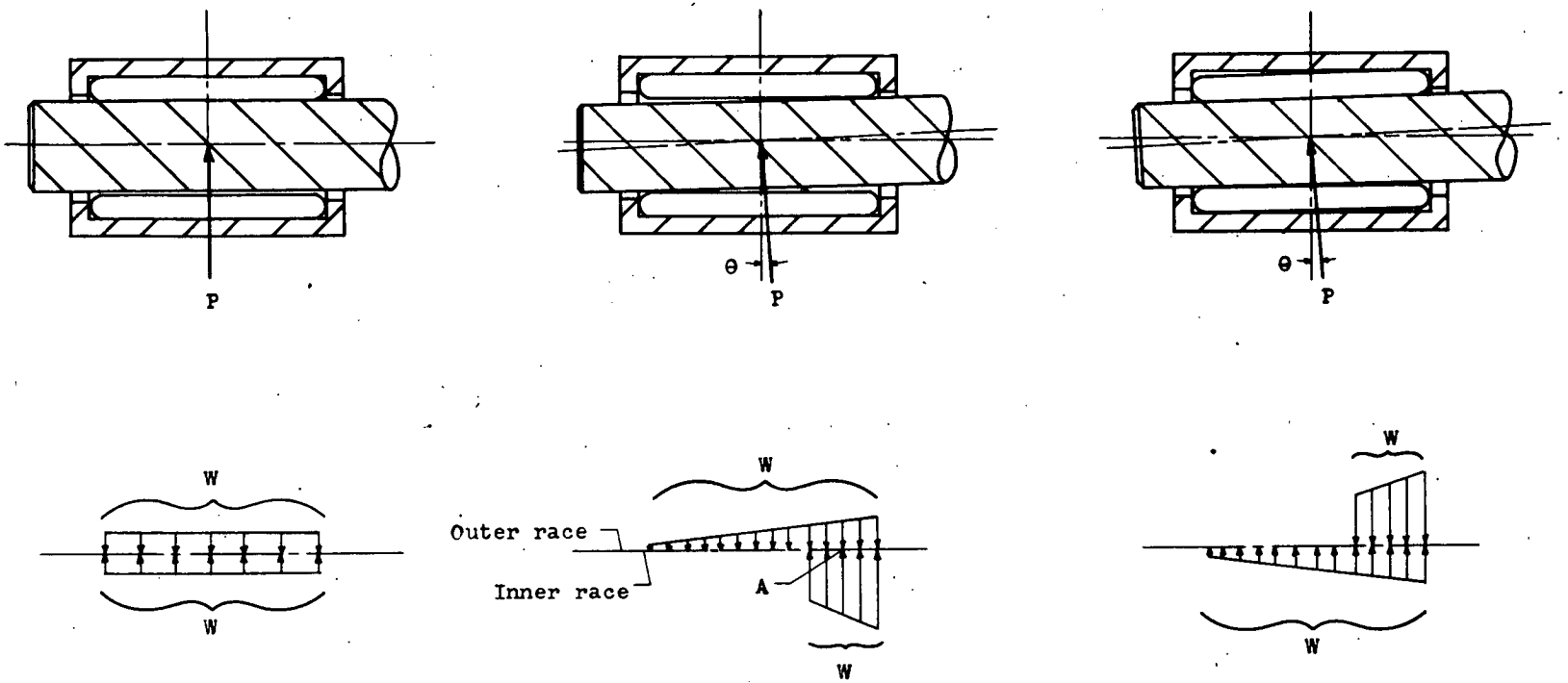

(a) No shaft deflection.

(b) Shaft deflection with needle parallel to outer race.

(c) Shaft deflection with needle parallel to inner race.

Figure 4. - Stress distribution and position of rolling elements in needle bearing with and without shaft deflection and without shaft rotation.

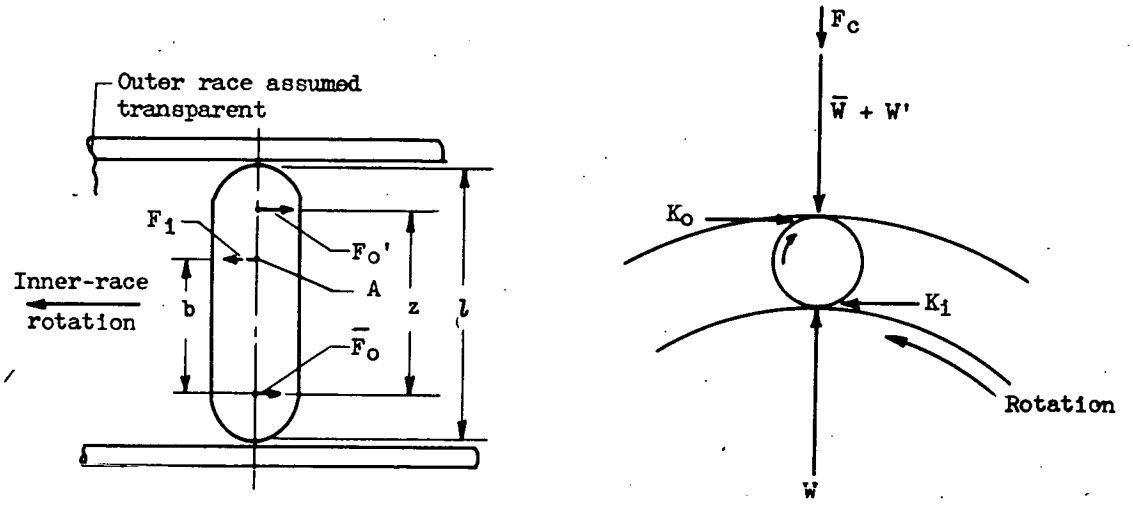

(a) Needle parallel to races.

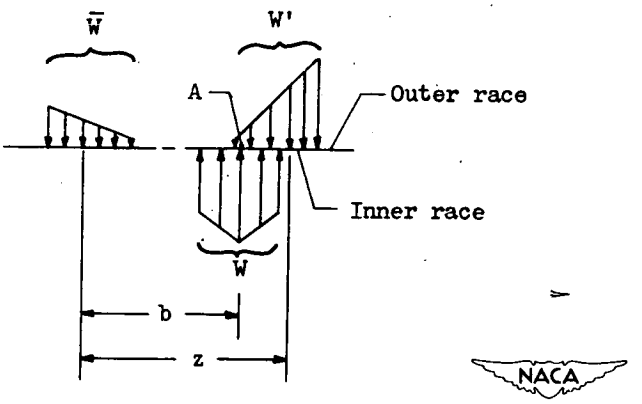

(b) Stress distribution between needle and races along length of skewed needle.

Figure 5. - Forces acting on straight and skewed needles.

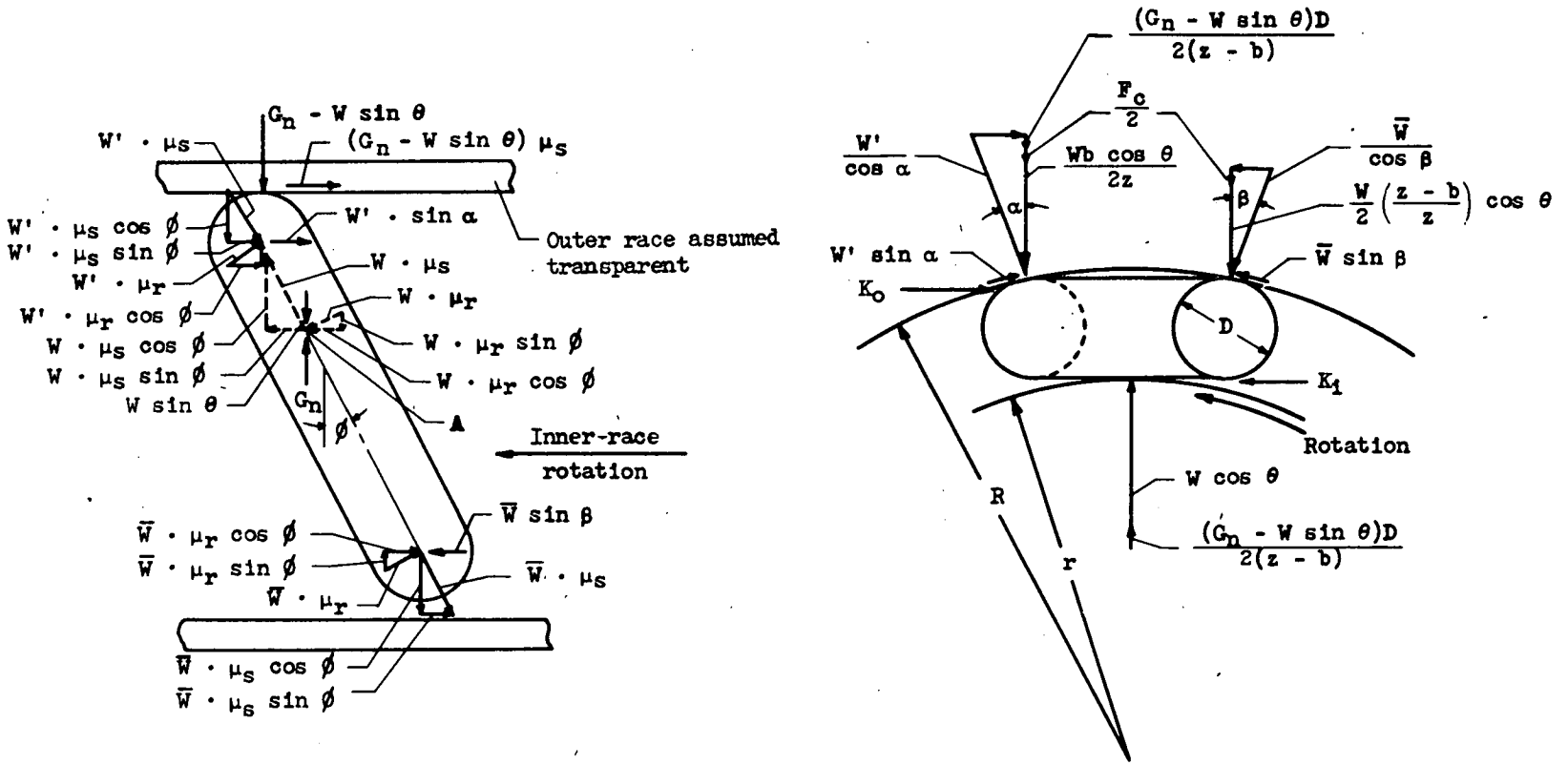

(c) Needle skewed.

Figure 5. - Continued. Forces acting on straight and skewed needles.

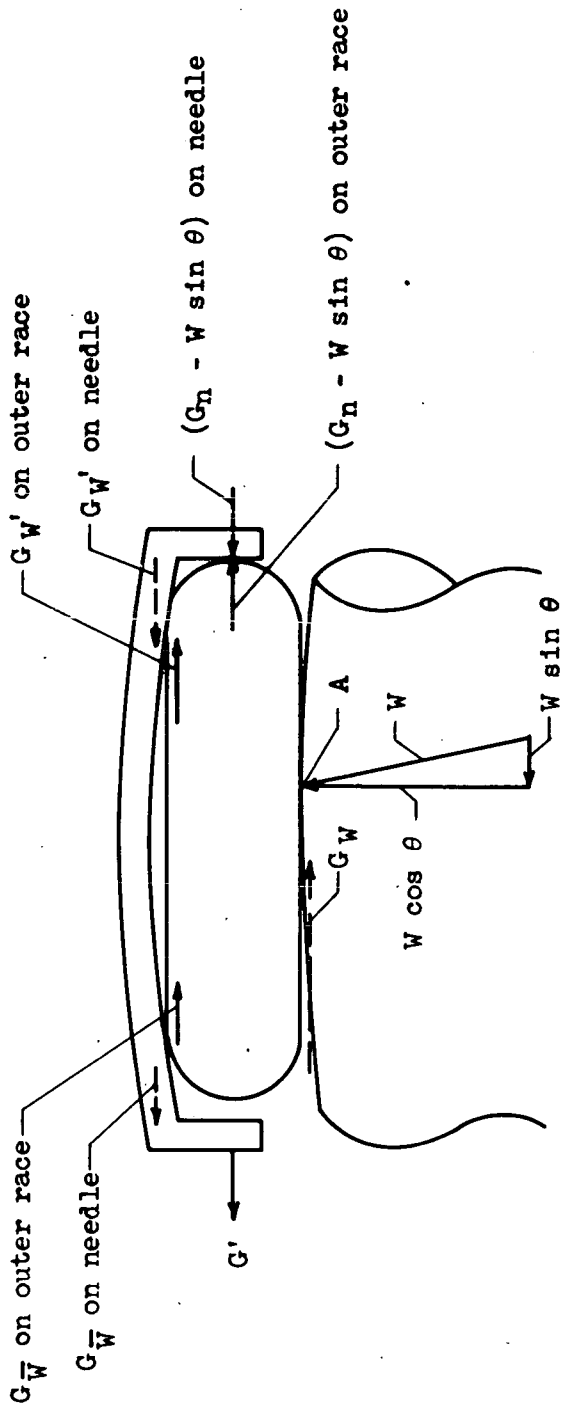

(d) Resultant end-thrust force.

Figure 5. - Concluded. Forces acting on straight and skewed needles.

Page intentionally left blank

Page intentionally left blank

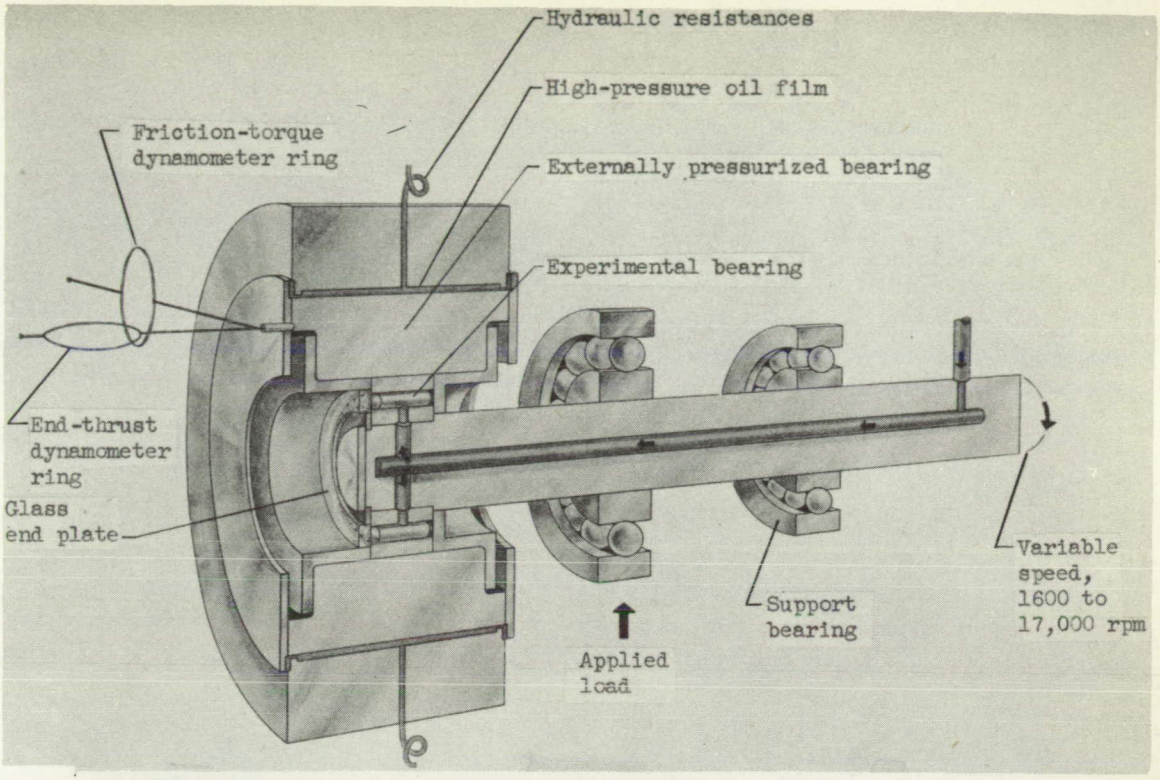

(a) Schematic diagram of experimental-shaft assembly.

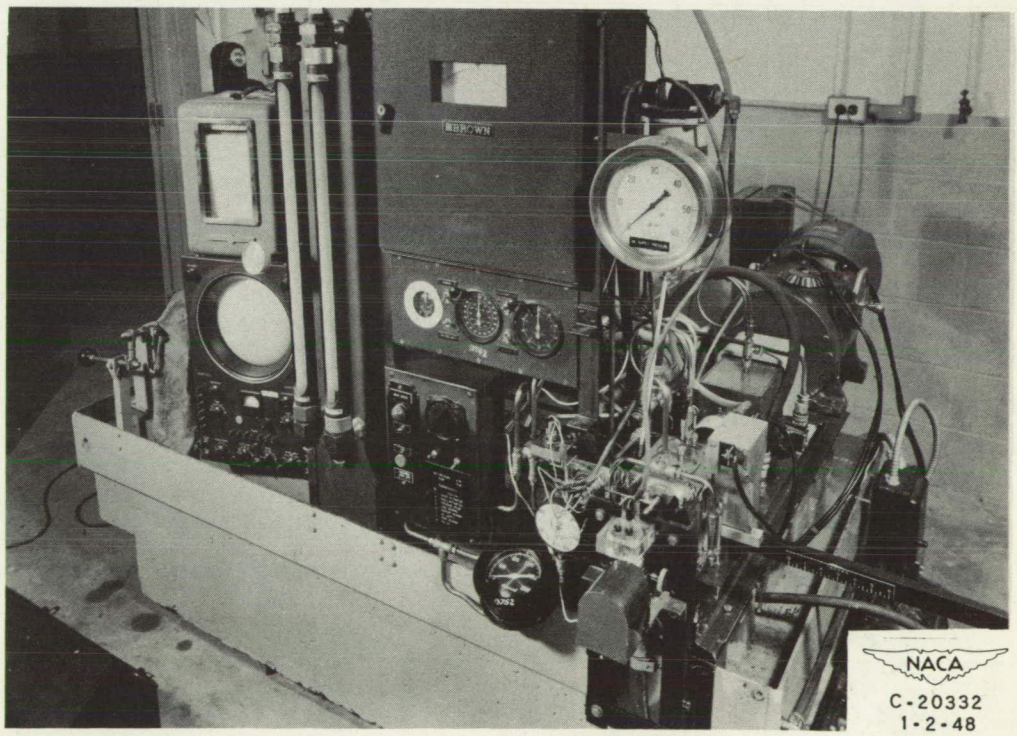

(b) Photograph of assembly.

Figure 6. - Needle-bearing test rig.

Page intentionally left blank

Page intentionally left blank

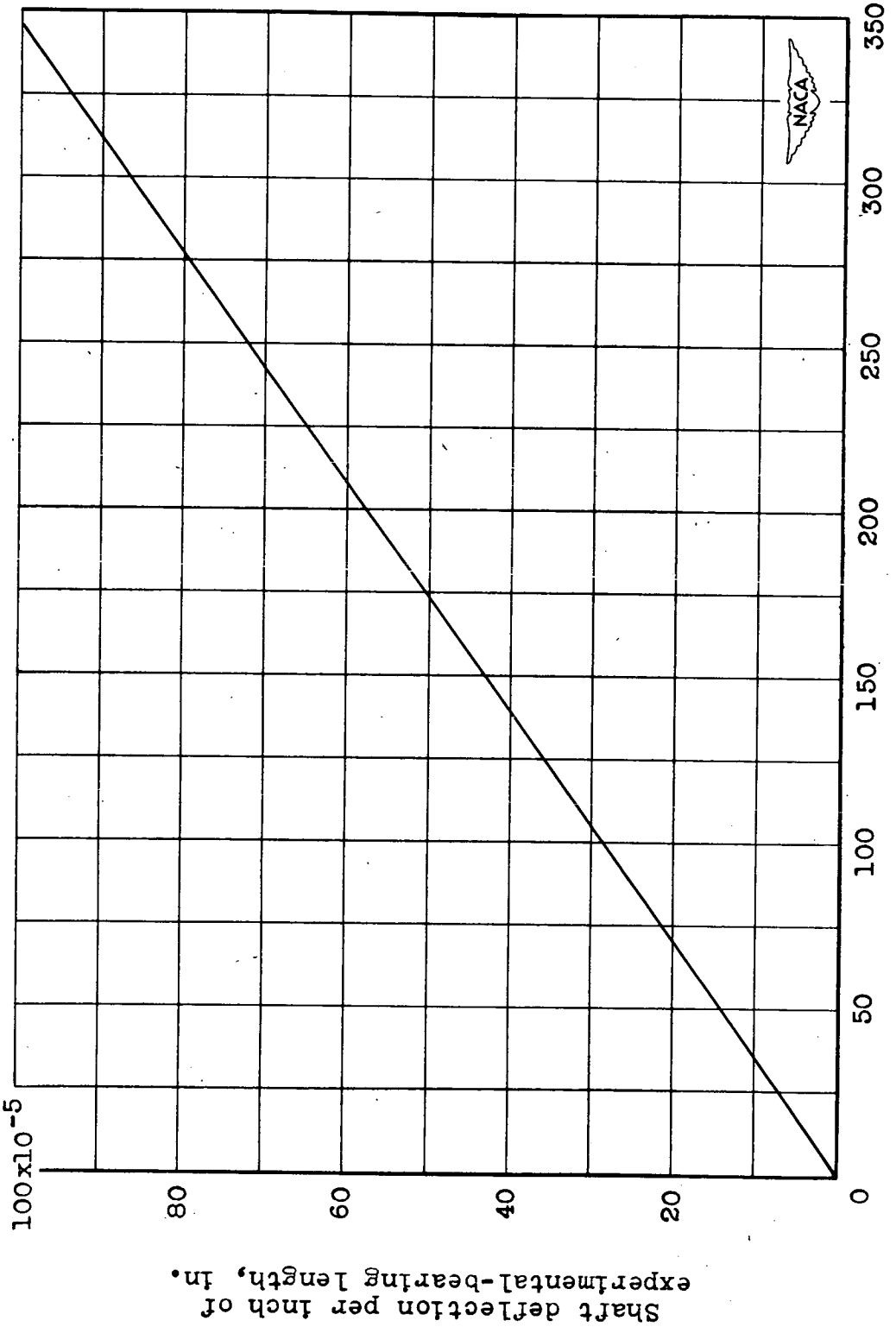

Figure 7. - Variation of shaft deflection with load.

Page intentionally left blank

Page intentionally left blank

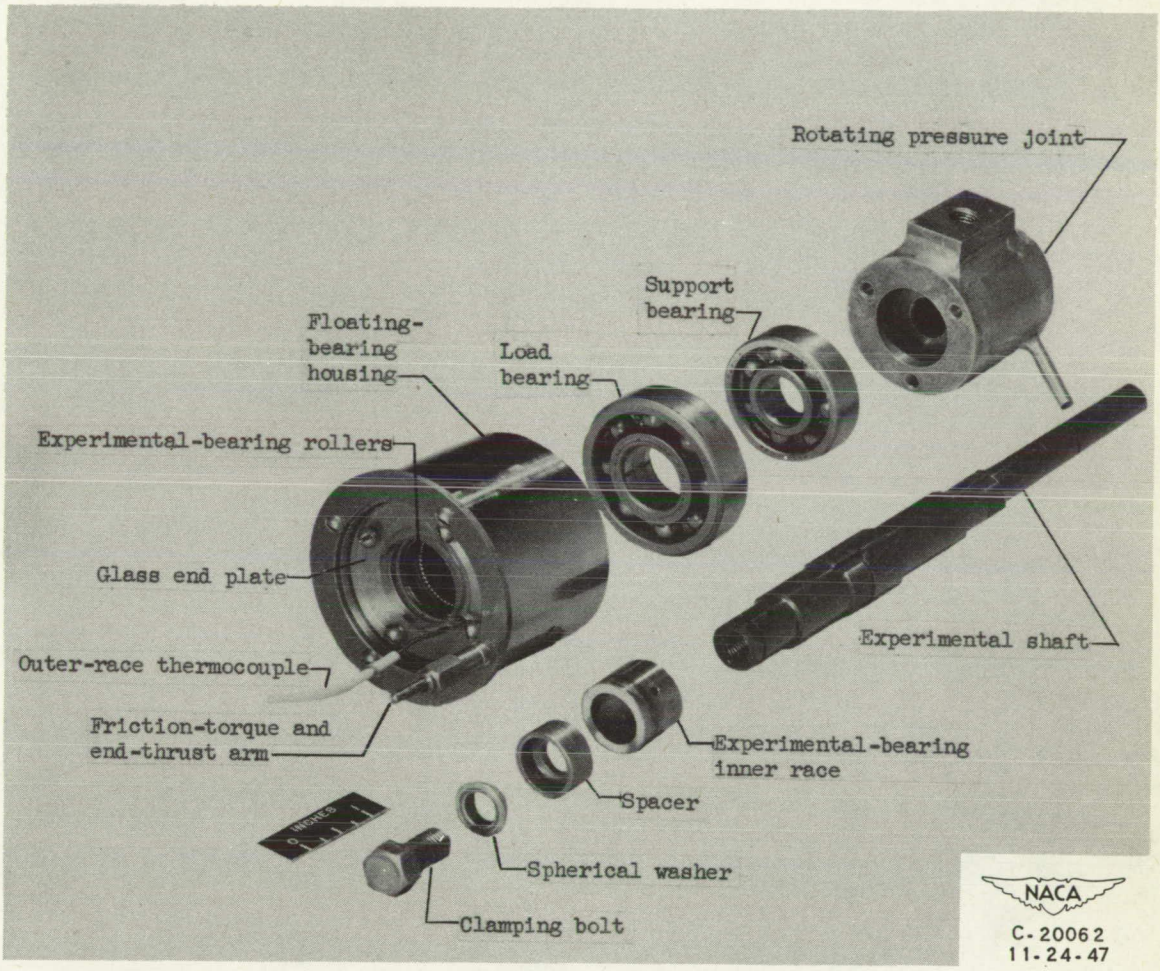

Figure 8. - Experimental-shaft assembly.

Page intentionally left blank

Page intentionally left blank

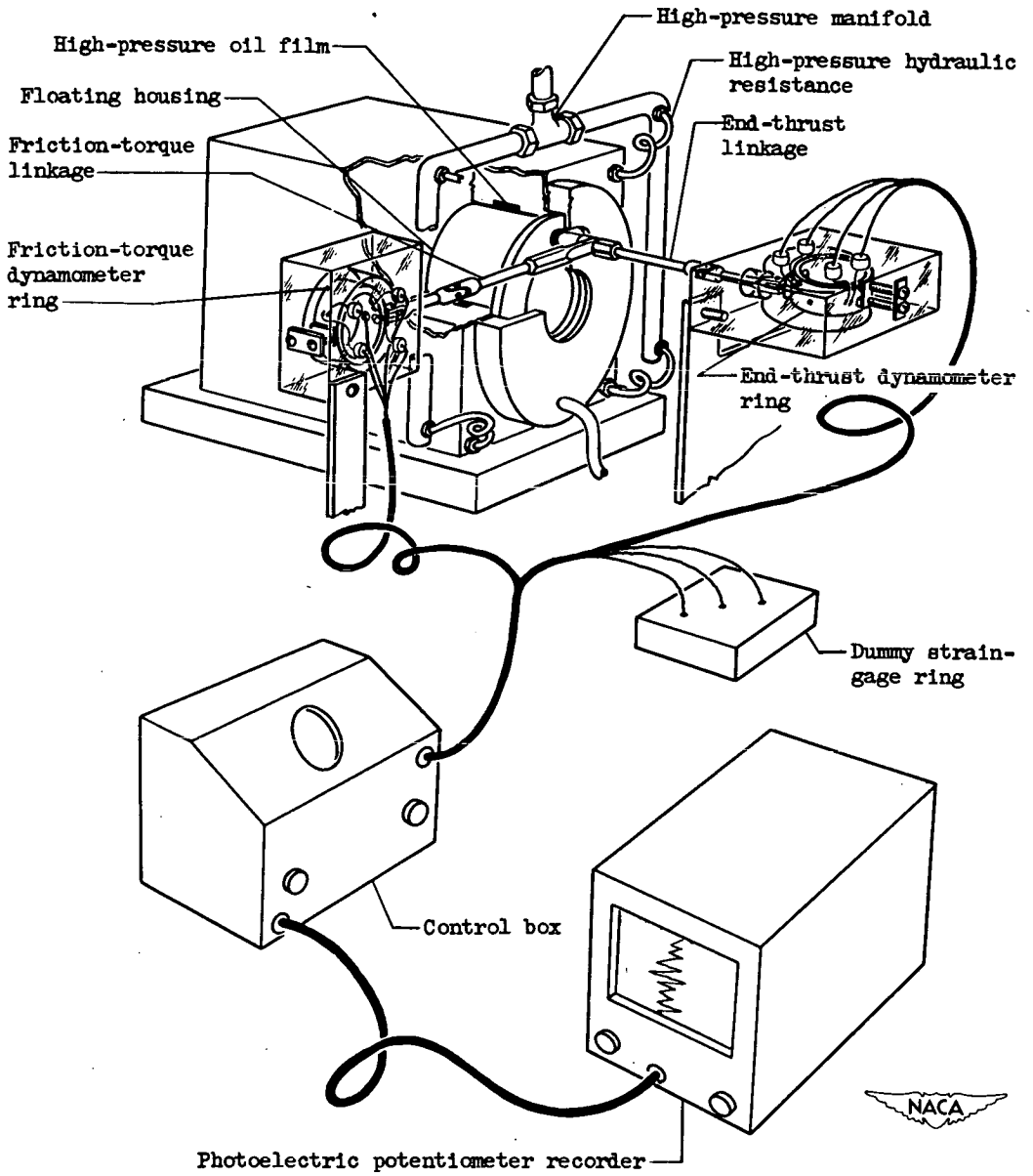

Figure 9. - Apparatus for determining end thrust and friction torque.

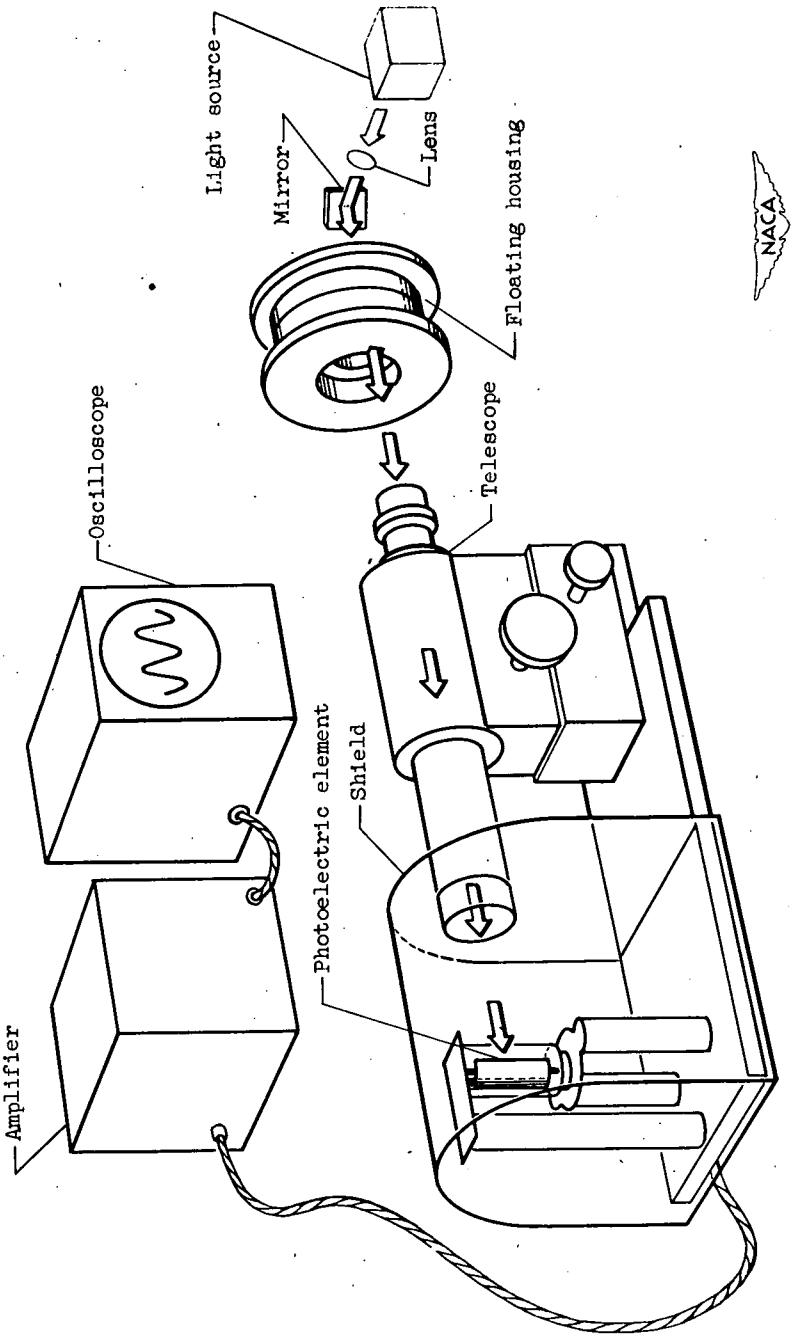

Figure 10. - Photoelectric apparatus for determining orbital speed of bearing needles.

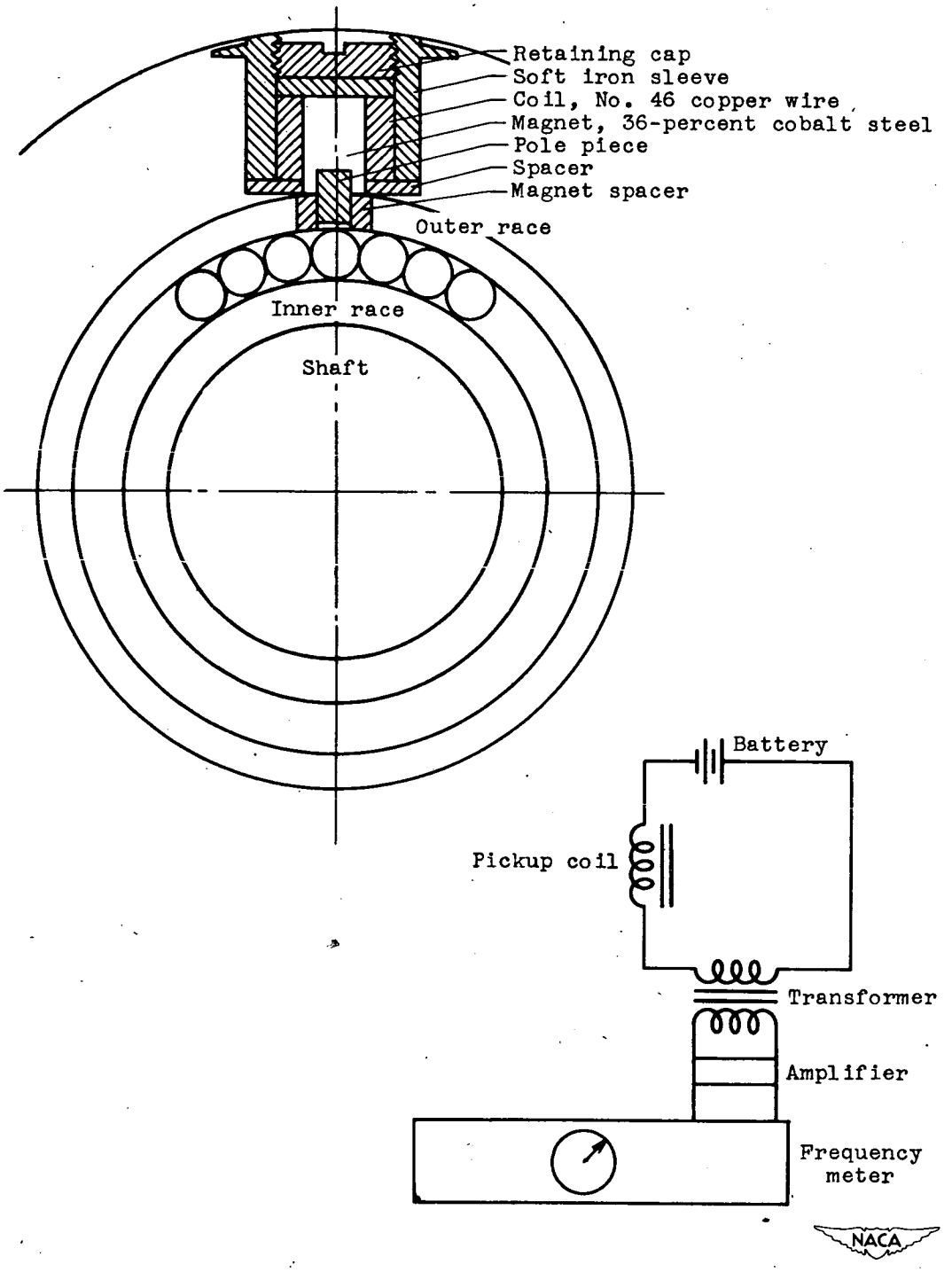

Figure 11. - Magnetic pickup apparatus for determining orbital speed.

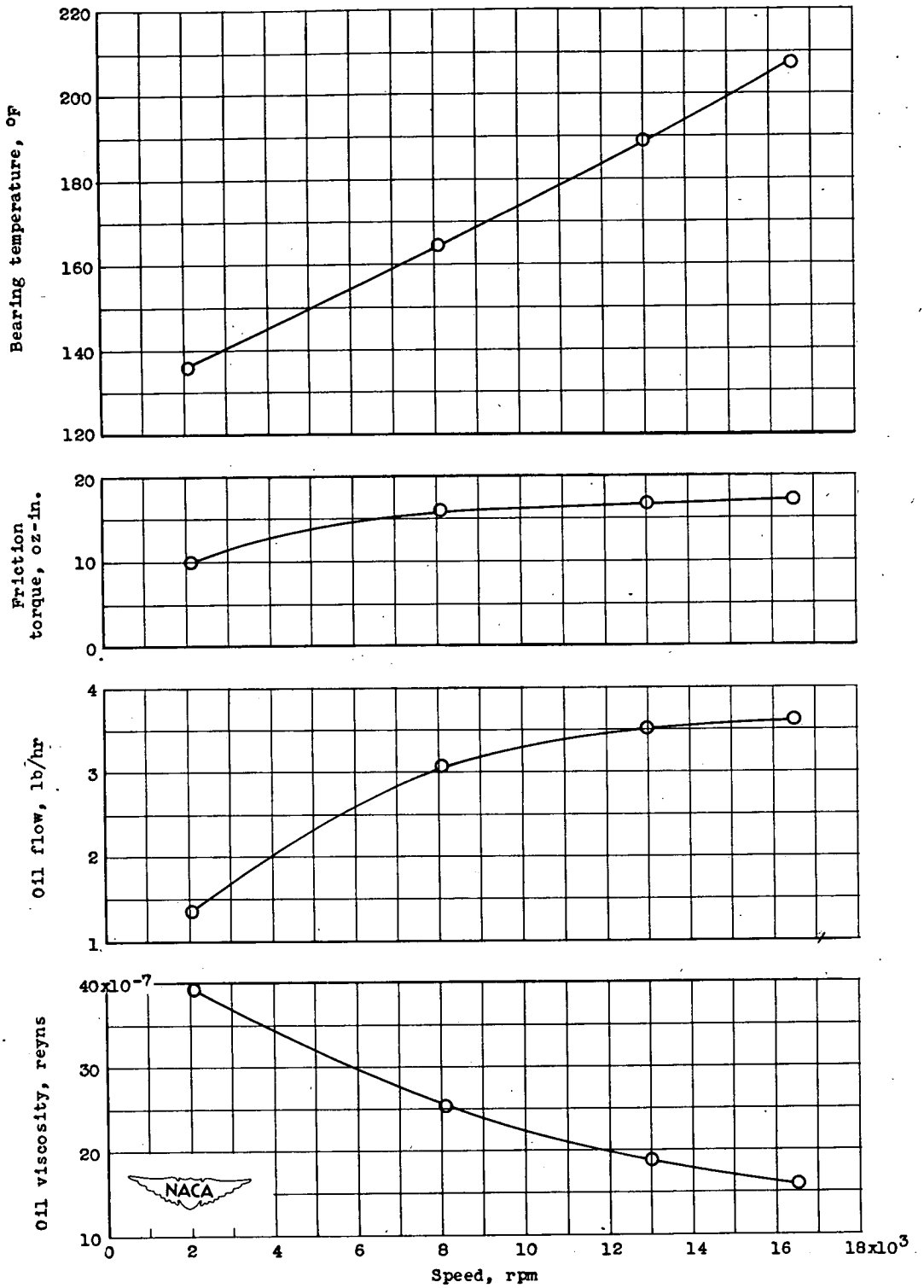

Figure 12. - Effect of speed on operating characteristics of copper-lead sleeve bearing. Bore, 1.118 inches; length-diameter ratio, 0.67; diametral clearance, 0.0024 inch; load, 200 pounds per square inch; oil-inlet pressure, 40 pounds per square inch; oil temperature at inlet to shaft, 85° F.

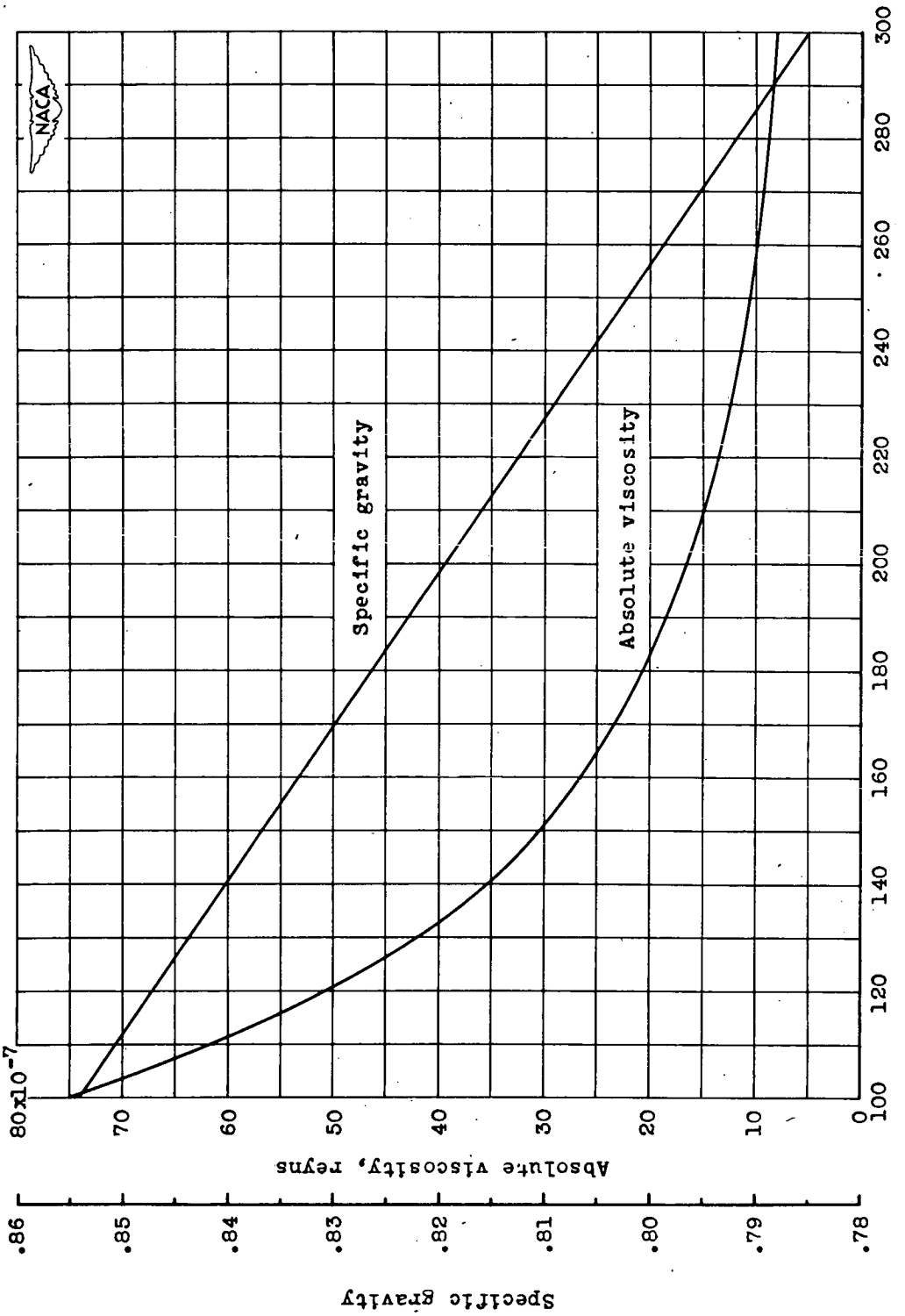

Figure 13. - Absolute viscosity and specific gravity of oil. Pour point, -50° F; flash point, 310° F; viscosity index, 155.

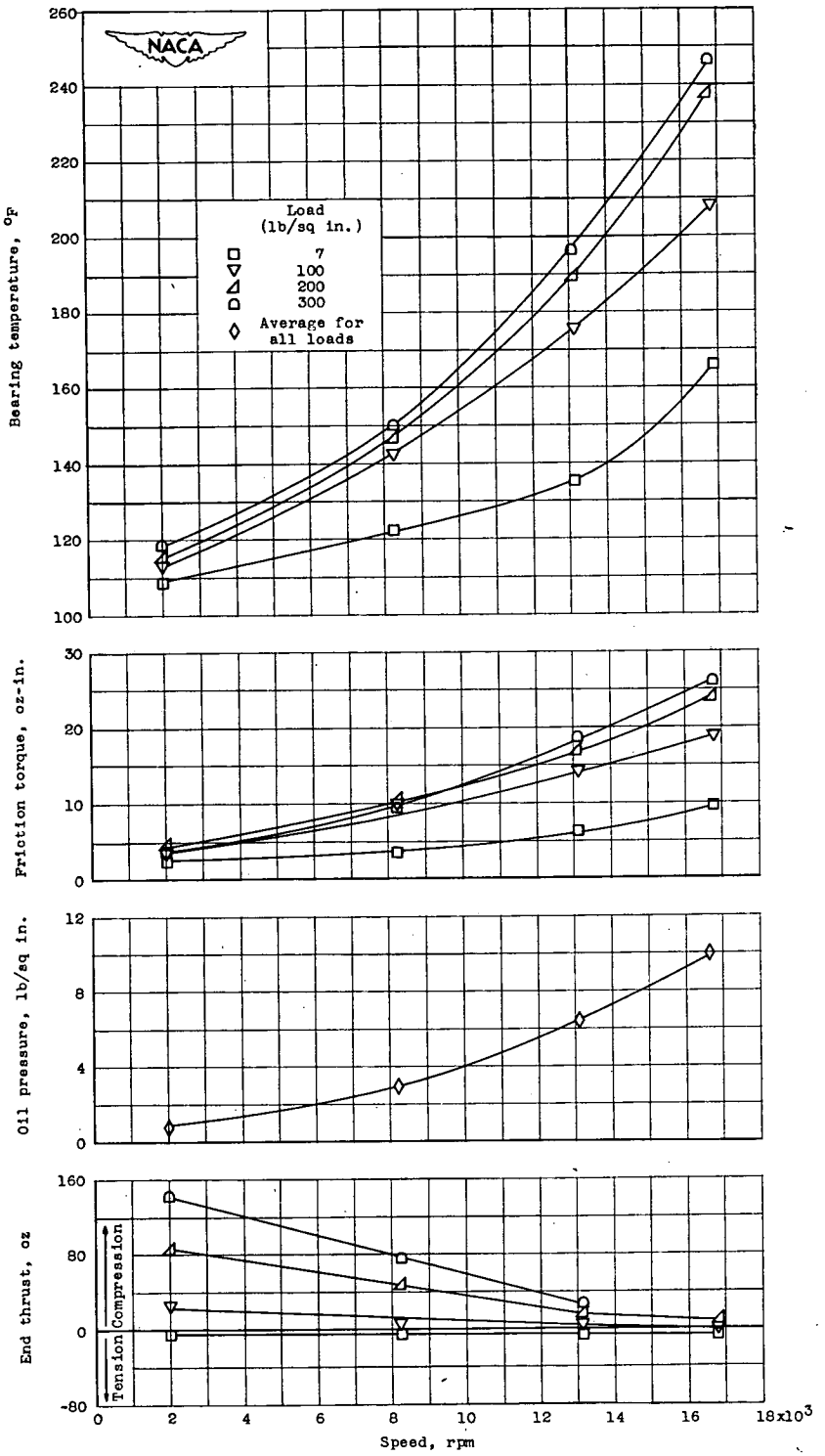

(a) Needle bearing 2: pitch diameter, 1.137 inches; effective length-diameter ratio of needles, 2.75; needle diameter, 0.137 inch; diametral clearance, 0.0010 inch; oil flow, 2 pounds per hour.

Figure 14. - Effect of speed on operating characteristics of needle bearings.

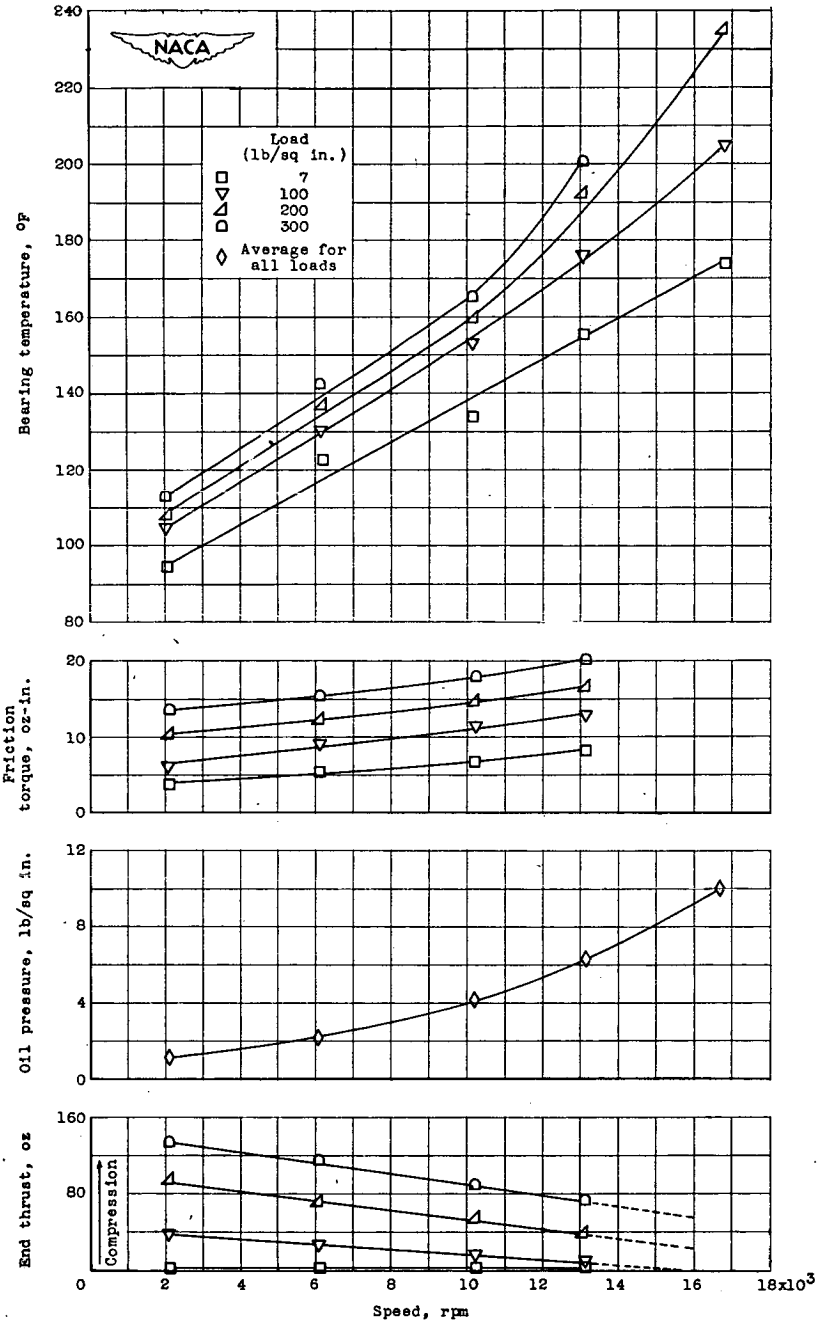

(b) Needle bearing 3; pitch diameter, 1.116 inches; effective length-diameter ratio of needles, 2.75; needle diameter, 0.1249 inch; diametral clearance, 0.0018 inch; oil flow, 2 pounds per hour.

Figure 14. - Continued. Effect of speed on operating characteristics of needle bearings.

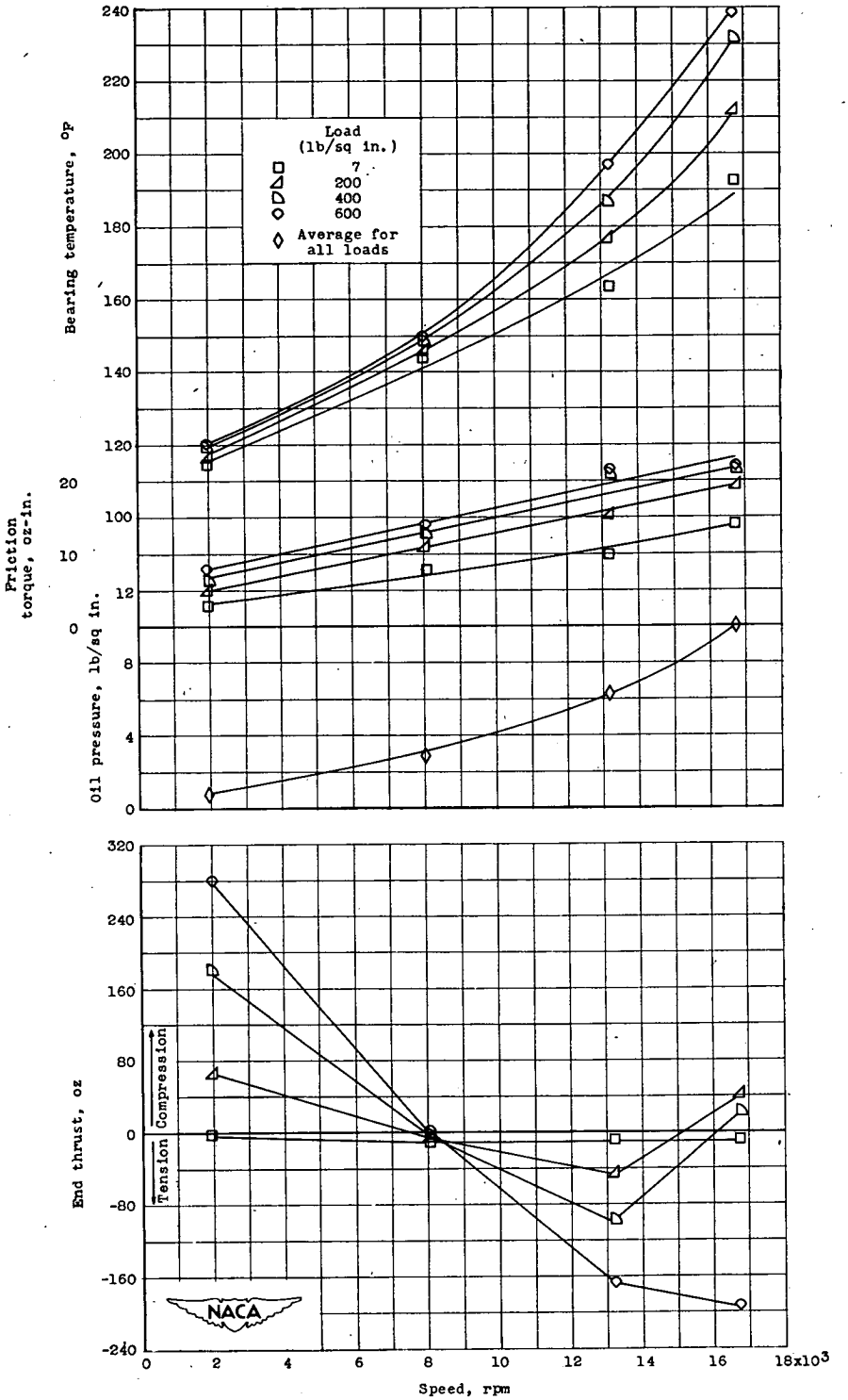

(c) Needle bearing 4; pitch diameter, 1.116 inches; effective length-diameter ratio of needles, 2.75; needle diameter, 0.1249 inch; diametral clearance, 0.0025 inch; oil flow, 2 pounds per hour.

Figure 14. - Continued. Effect of speed on operating characteristics of needle bearings.

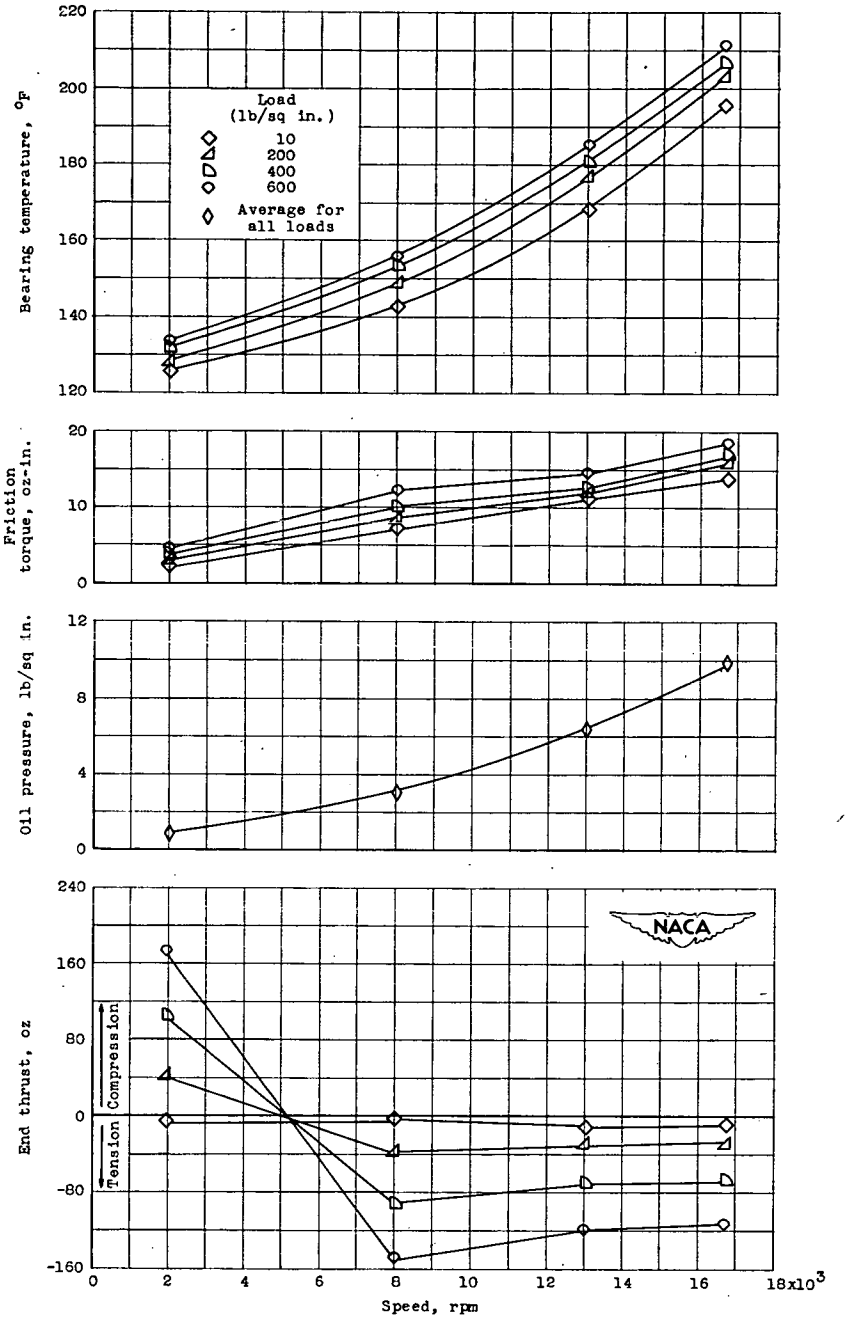

(d) Needle bearing 7; pitch diameter, 1.117 inches; effective length-diameter ratio of needles, 3.50; needle diameter, 0.0625 inch; diametral clearance, 0.0016 inch; oil flow, 0.5 pound per hour.

Figure 14. - Continued. Effect of speed on operating characteristics of needle bearings.

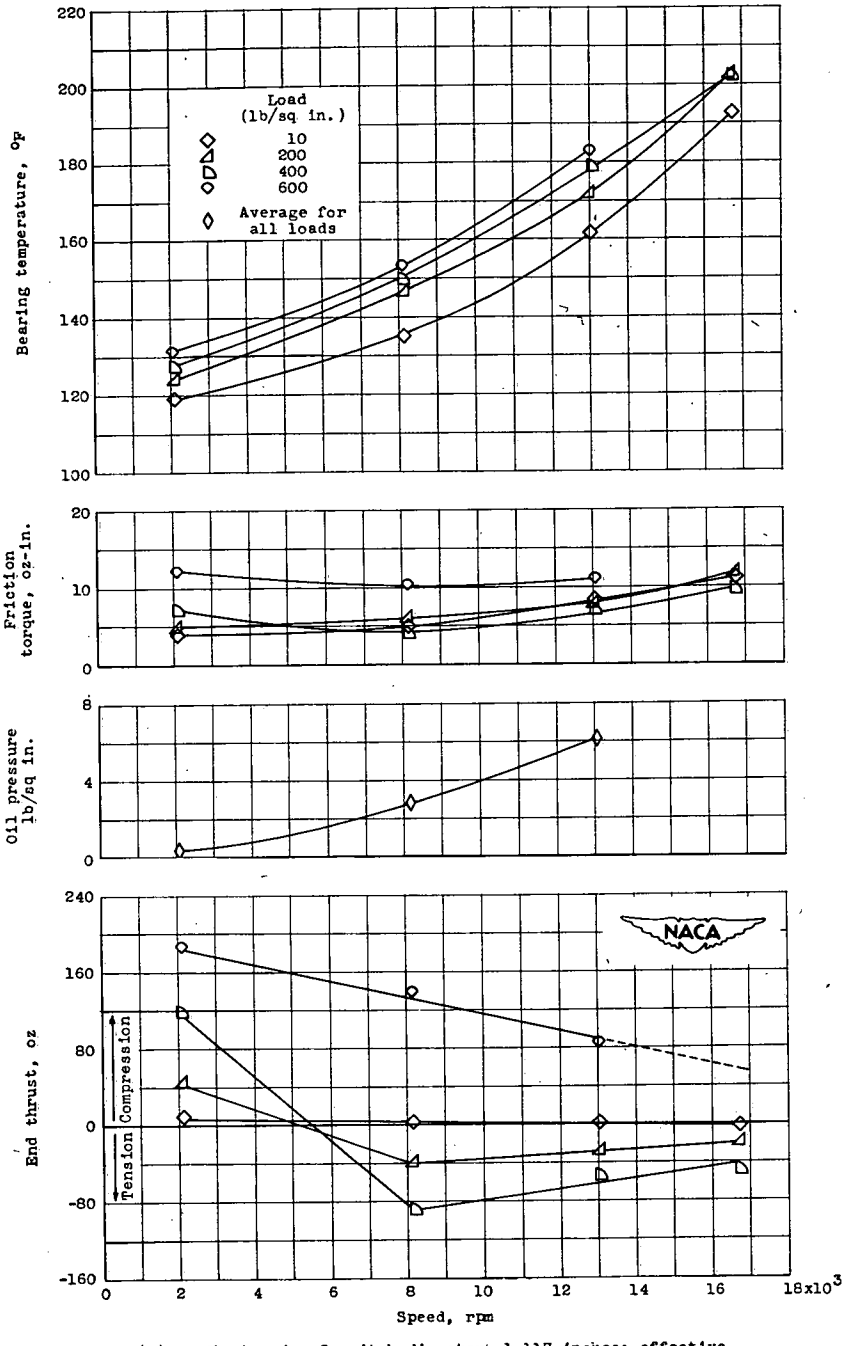

(e) Needle bearing 8; pitch diameter, 1.117 inches; effective length-diameter ratio of needles, 3.50; needle diameter, 0.0625 inch; diametral clearance, 0.0028 inch; oil flow, 0.5 pound per hour.

Figure 14. - Continued. Effect of speed on operating characteristics of needle bearings.

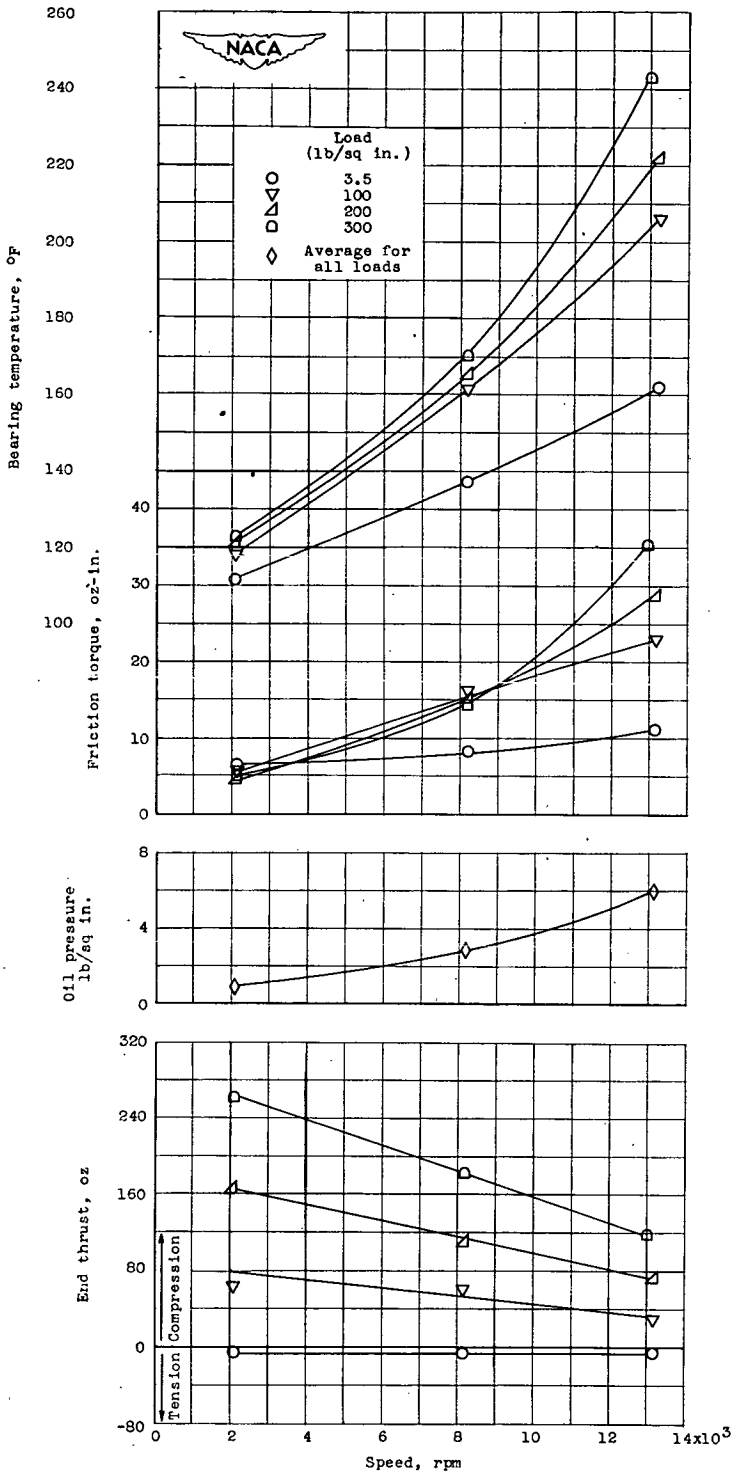

(f) Needle bearing 9; pitch diameter, 1.117 inches; effective length-diameter ratio of needles, 11.67; needle diameter, 0.0624 inch; diametral clearance, 0.0017 inch; oil flow, 2 pounds per hour.

Figure 14. - Continued. Effect of speed on operating characteristics of needle bearings.

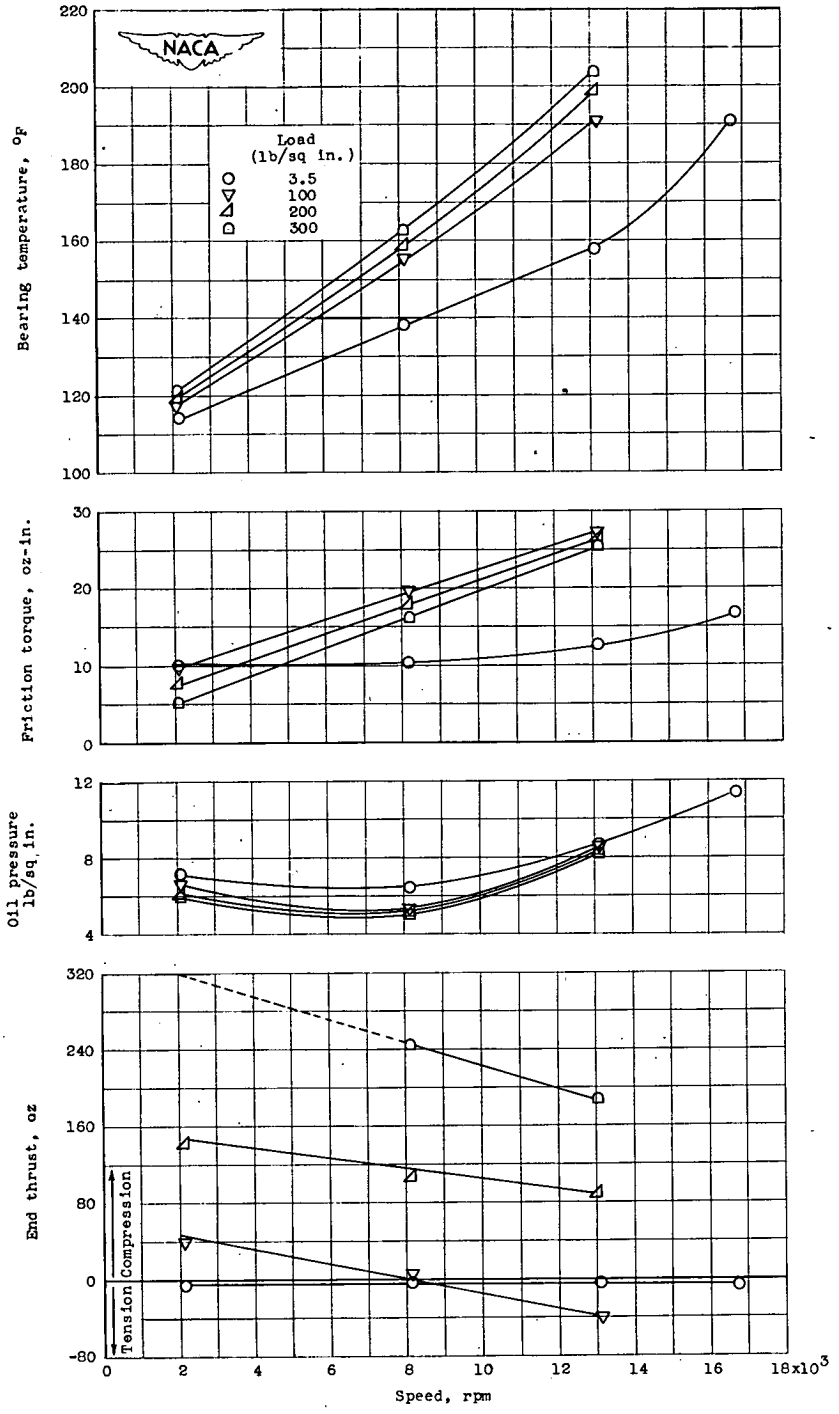

(g) Needle bearing 10; pitch diameter, 1.117 inches; effective length-diameter ratio of needles, 11.67; needle diameter, 0.0625 inch; diametral clearance, 0.0027 inch; oil flow, 12 pounds per hour.

Figure 14. - Concluded. Effect of speed on operating characteristics of needle bearings.

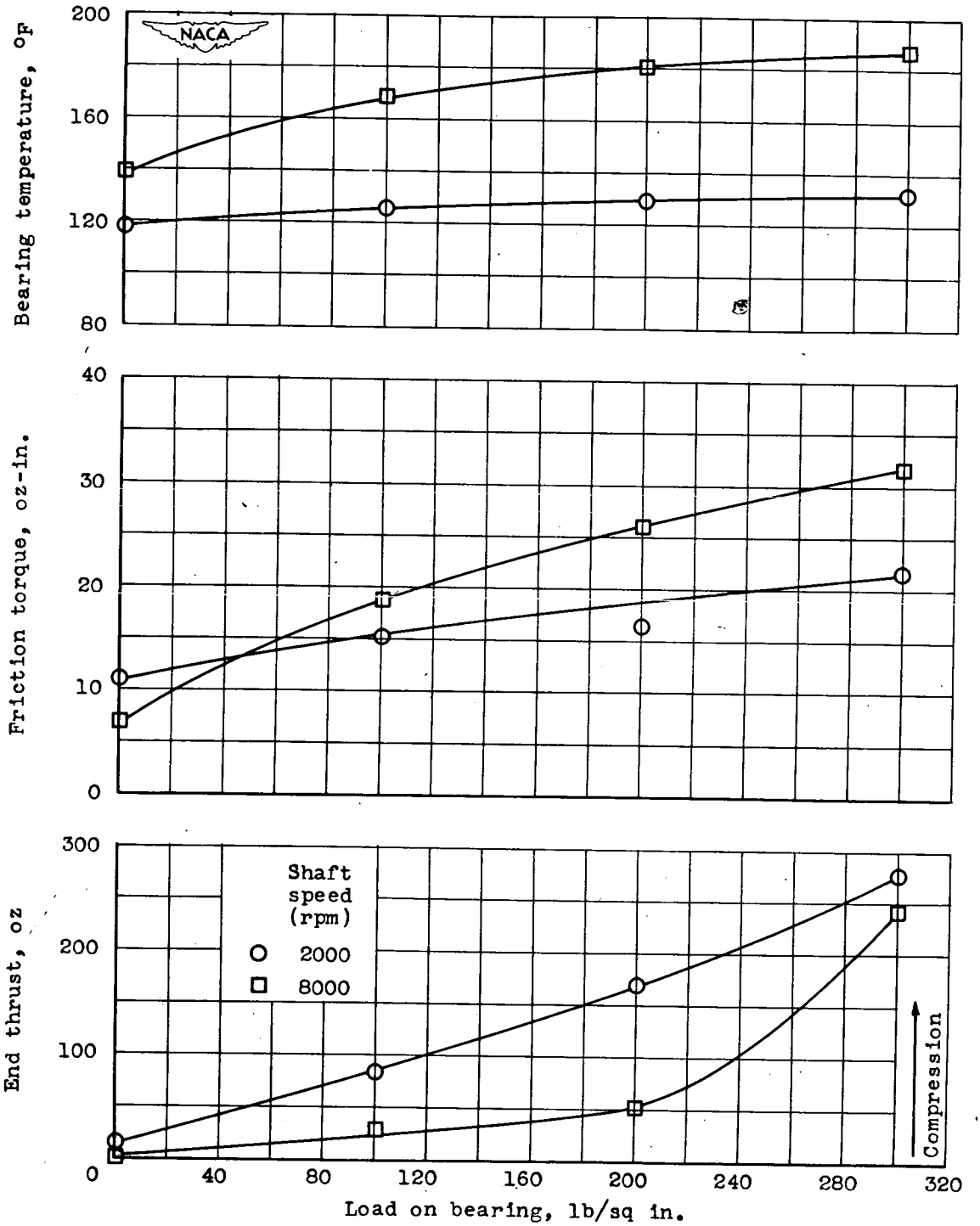

Figure 15. - Effect of load on operating characteristics of needle bearing 6. Pitch diameter, 1.116 inches; effective length-diameter ratio of needles, 5.71; needle diameter, 0.1248 inch; diametral clearance, 0.0020 inch; oil flow, 2 pounds per hour.

Page intentionally left blank

Page intentionally left blank

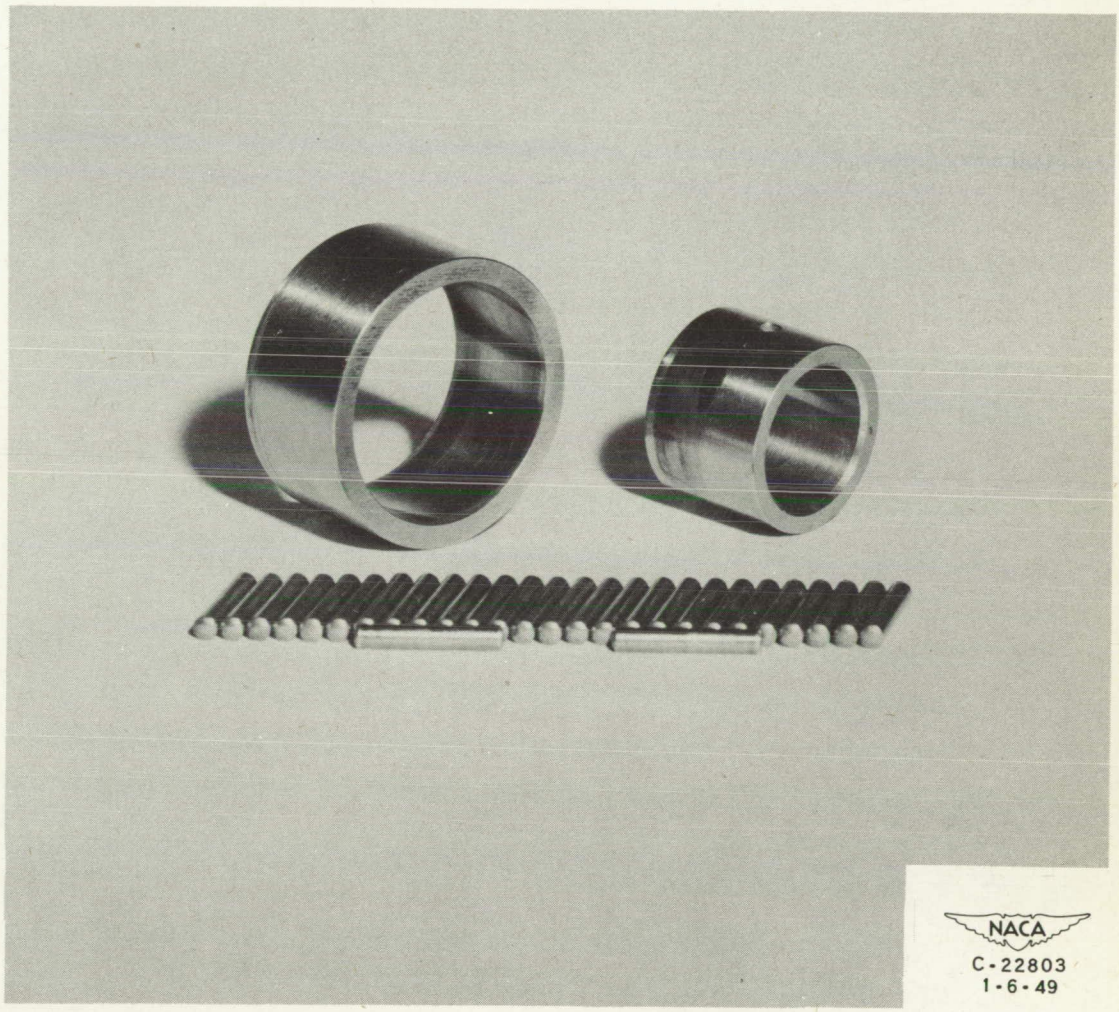

Figure 16. - Needle bearing 6 after investigation.

Page intentionally left blank

Page intentionally left blank

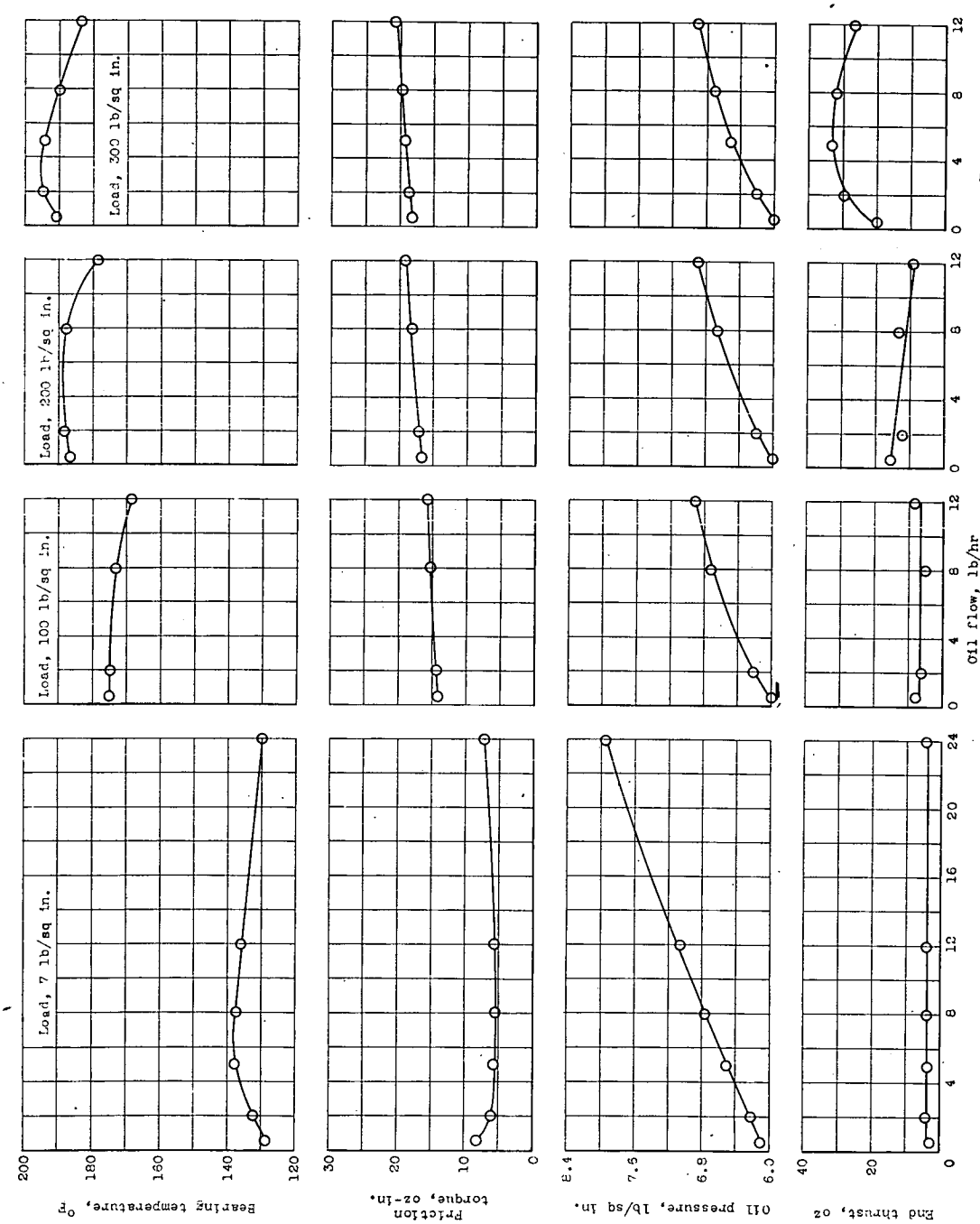

(a) Shaft speed, 13,000 rpm; load, 7, 100, 200, and 300 pounds per square inch.

Figure 17. - Effect of oil flow on operating characteristics of needle bearing 2. Pitch diameter, 1.137 inches; effective length-diameter ratio of needles, 2.75; needle diameter, 0.137 inch; diametrul clearance, 0.0010 inch.

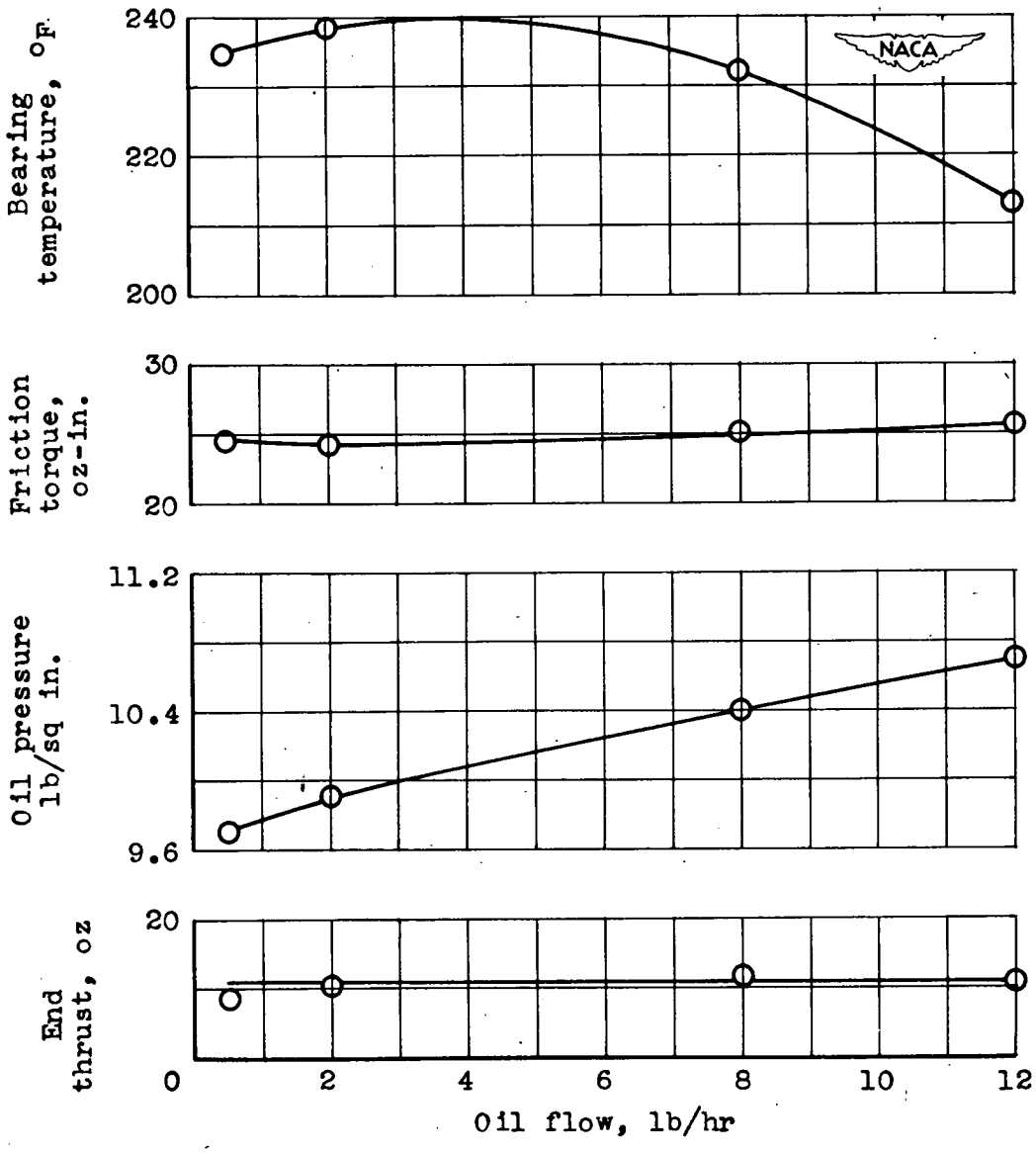

(b) Shaft speed, 16,700 rpm;
load, 200 pounds per square inch.

Figure 17. - Concluded. Effect of oil flow on operating characteristics of needle bearing 2. Pitch diameter, 1.137 inches; effective length-diameter ratio of needles, 2.75; needle diameter, 0.137 inch; diametral clearance, 0.0010 inch.

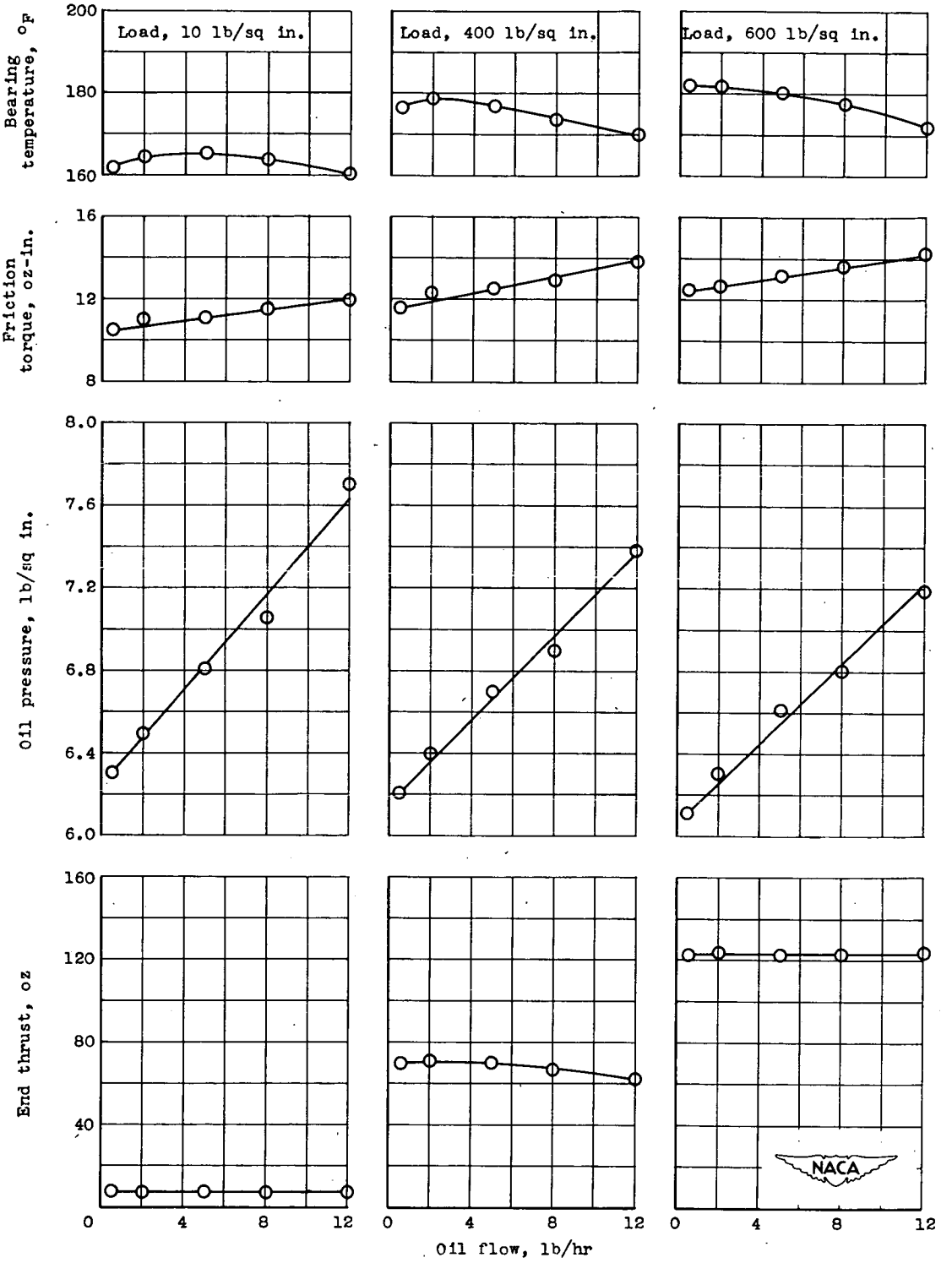

Figure 18. - Effect of oil flow on operating characteristics of needle bearing 7. Pitch diameter, 1.117 inches; effective length-diameter ratio of needles, 3.50; needle diameter, 0.0625 inch; diametral clearance, 0.0016 inch; speed, 13,000 rpm.

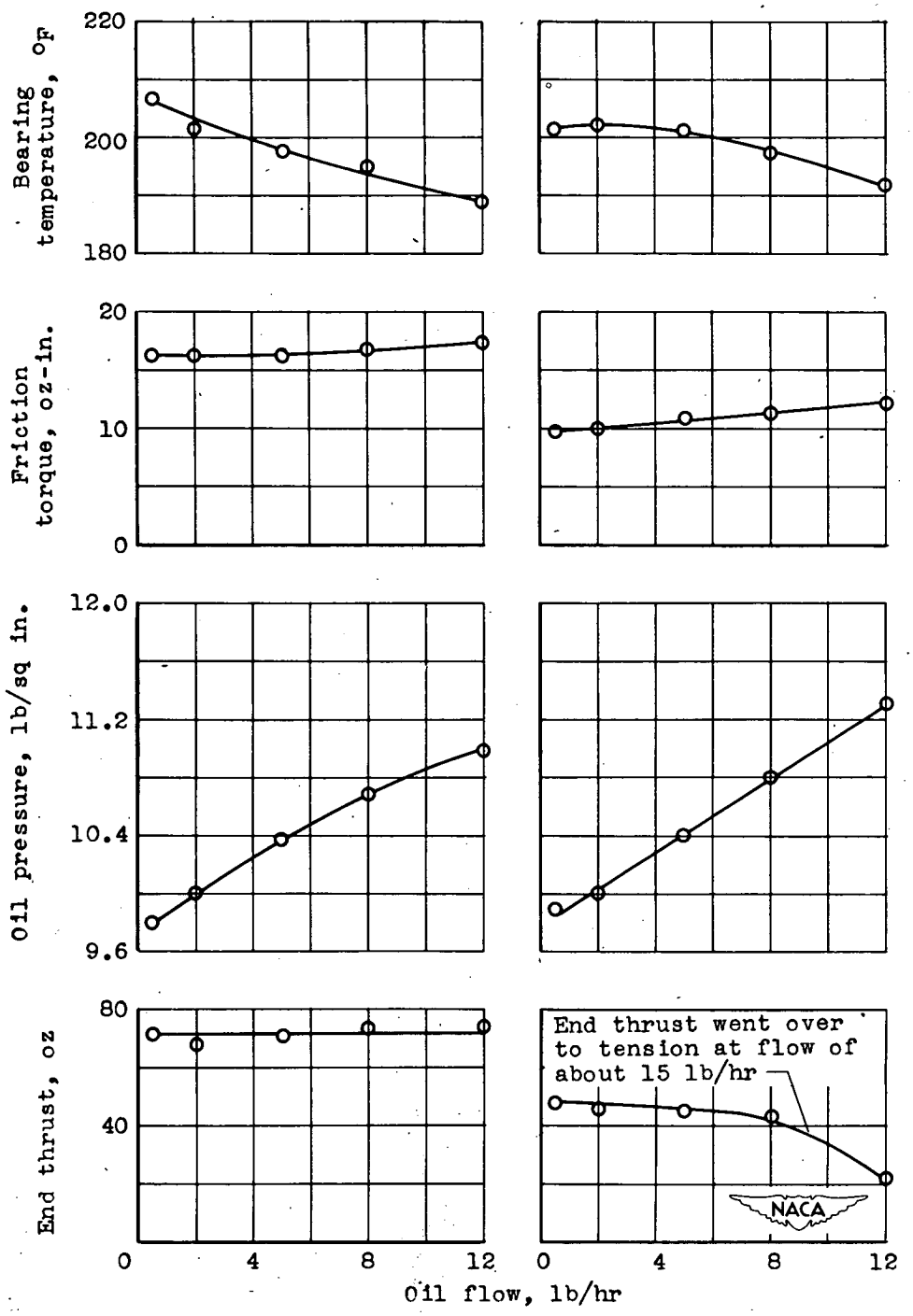

(a) Needle bearing 7; diametral clearance, 0.0016 inch.

(b) Needle bearing 8; diametral clearance, 0.0028 inch.

Figure 19. - Effect of oil flow on operating characteristics of needle bearings 7 and 8. Pitch diameter, 1.117 inches; effective length-diameter ratio of needles, 3.50; needle diameter, 0.0625 inch; speed, 16,600 rpm; load, 400 pounds per square inch.

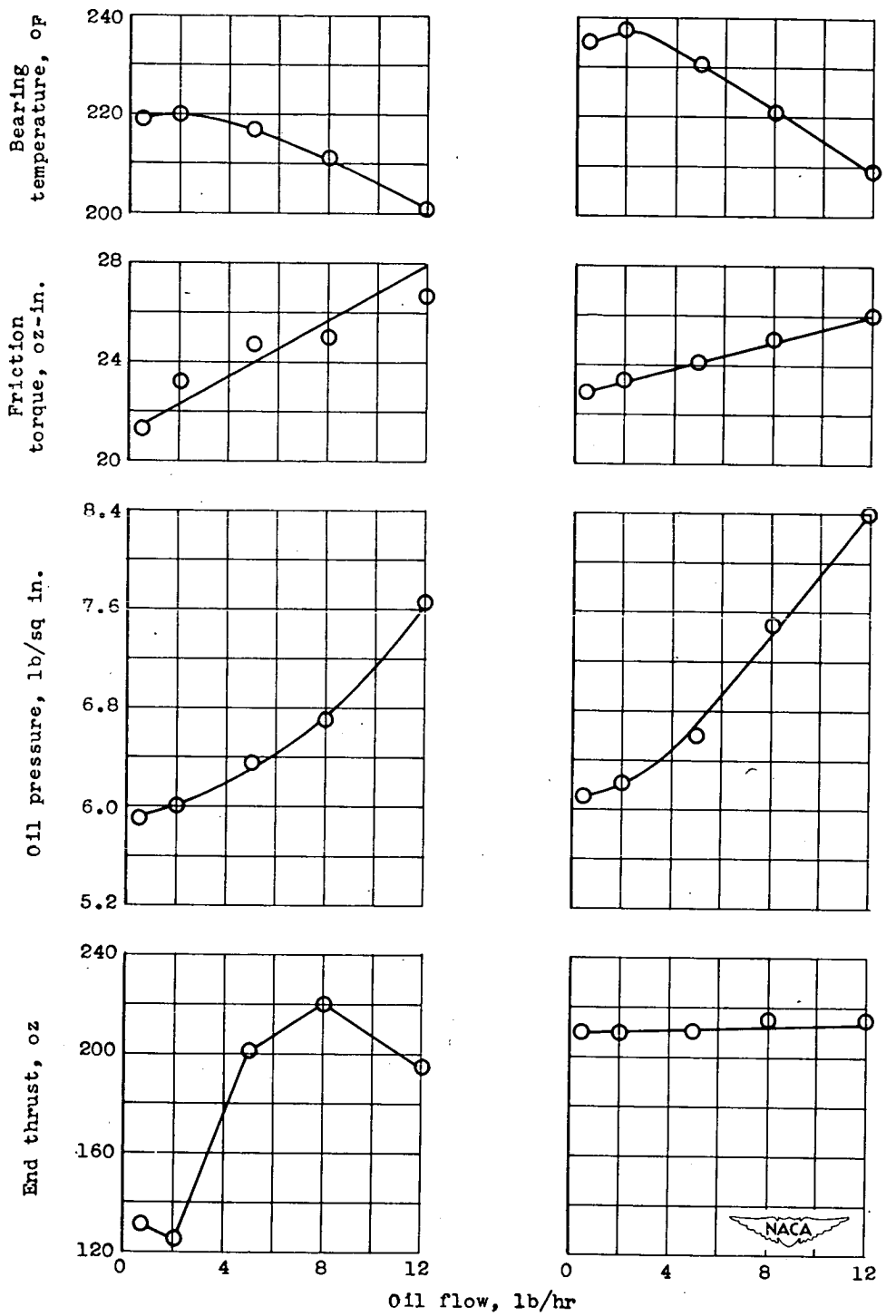

(a) Needle bearing 9; diametral clearance, 0.0017 inch; needle diameter, 0.0624 inch.

(b) Needle bearing 10; diametral clearance, 0.0027 inch; needle diameter, 0.0625 inch.

Figure 20. - Effect of oil flow on operating characteristics of needle bearings 9 and 10. Pitch diameter, 1.117 inches; effective length-diameter ratio of needles, 11.67; speed, 13,000 rpm; load, 300 pounds per square inch.

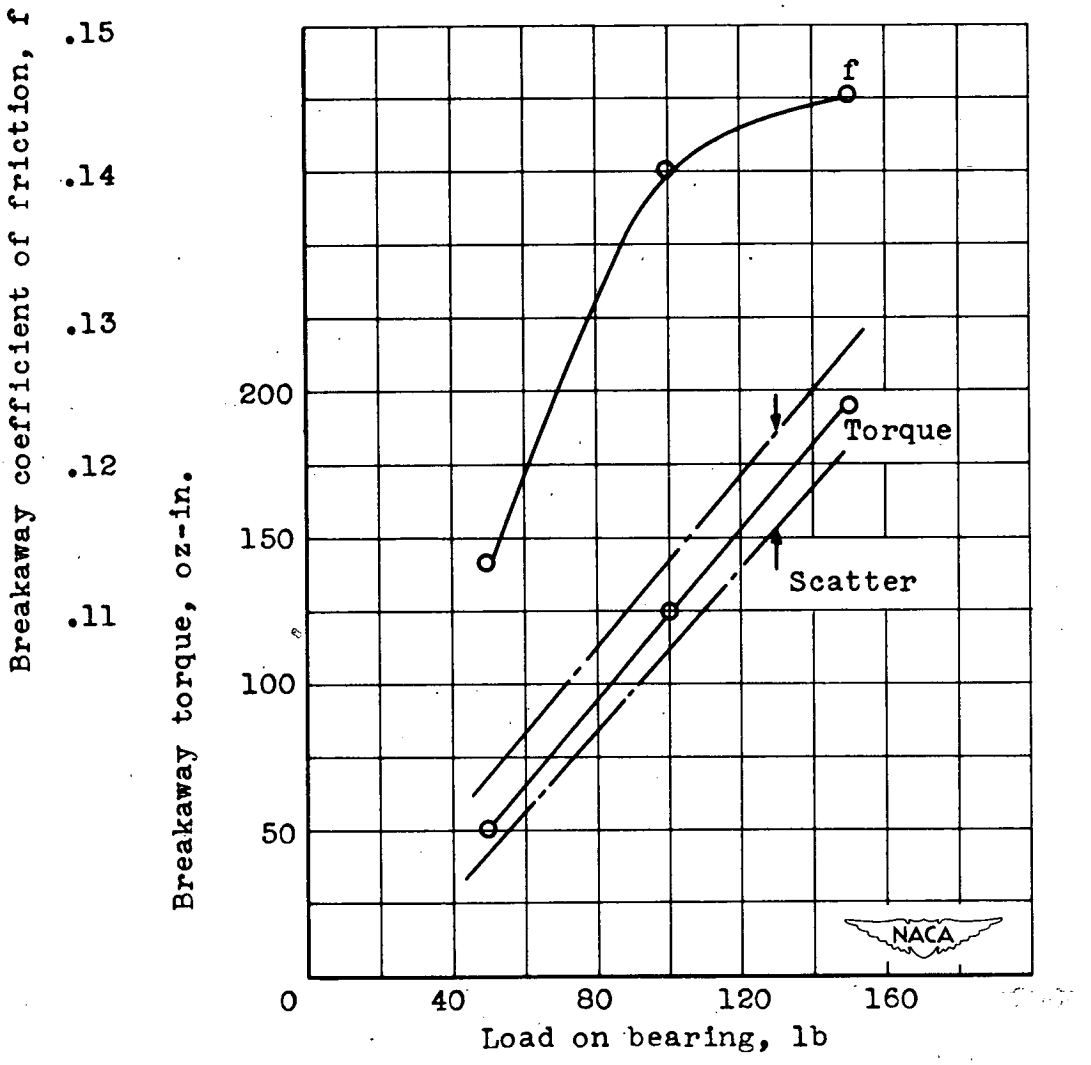

Figure 21. - Effect of load on breakaway torque of copper-lead sleeve bearing by spring-scale method. Bore, 1.118 inches; length-diameter ratio, 0.67; diametral clearance, 0.0024 inch.

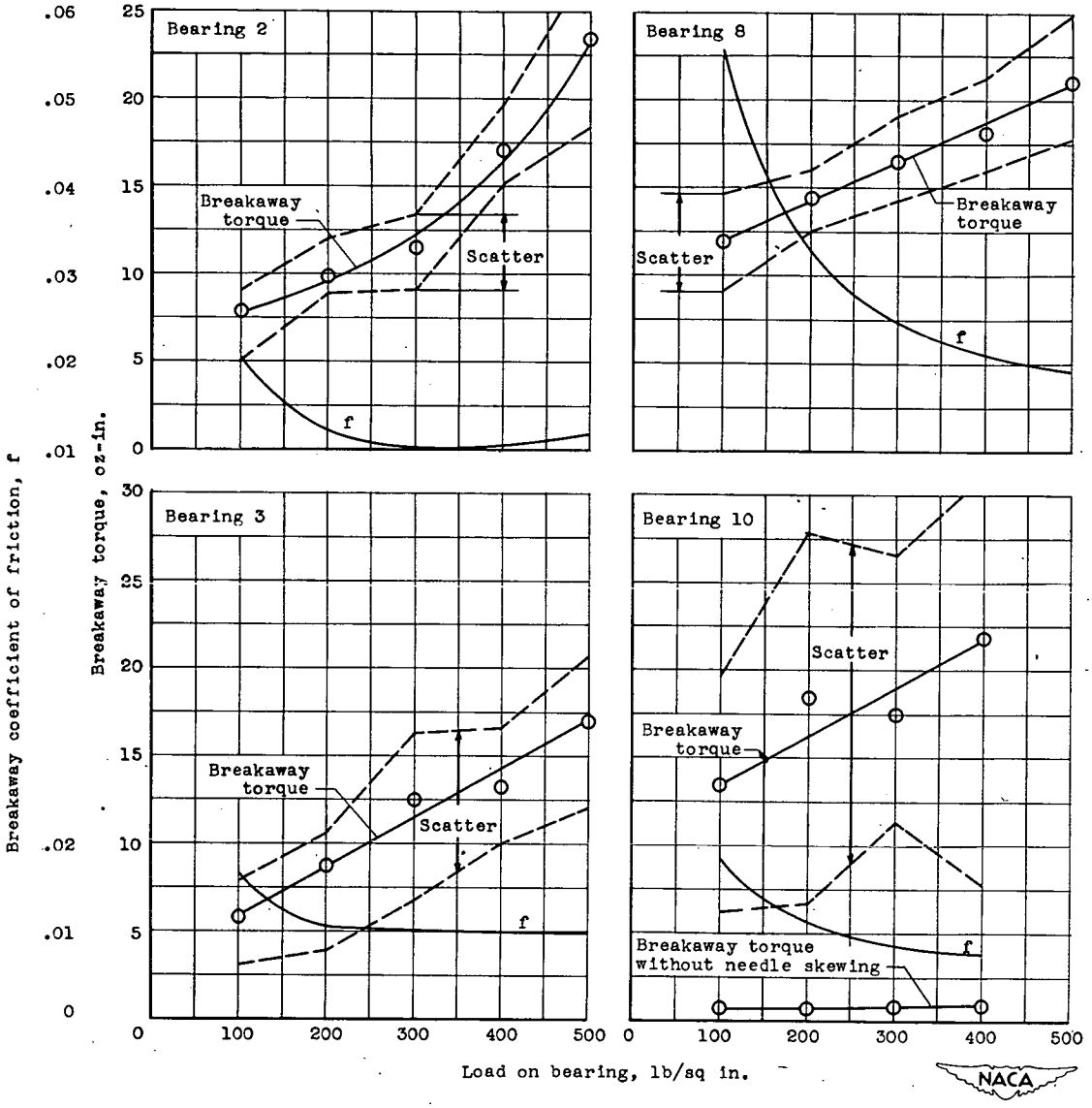

Figure 22. - Variation of breakaway torque and breakaway coefficient of friction for needle bearings 2, 3, 8, and 10 with load.

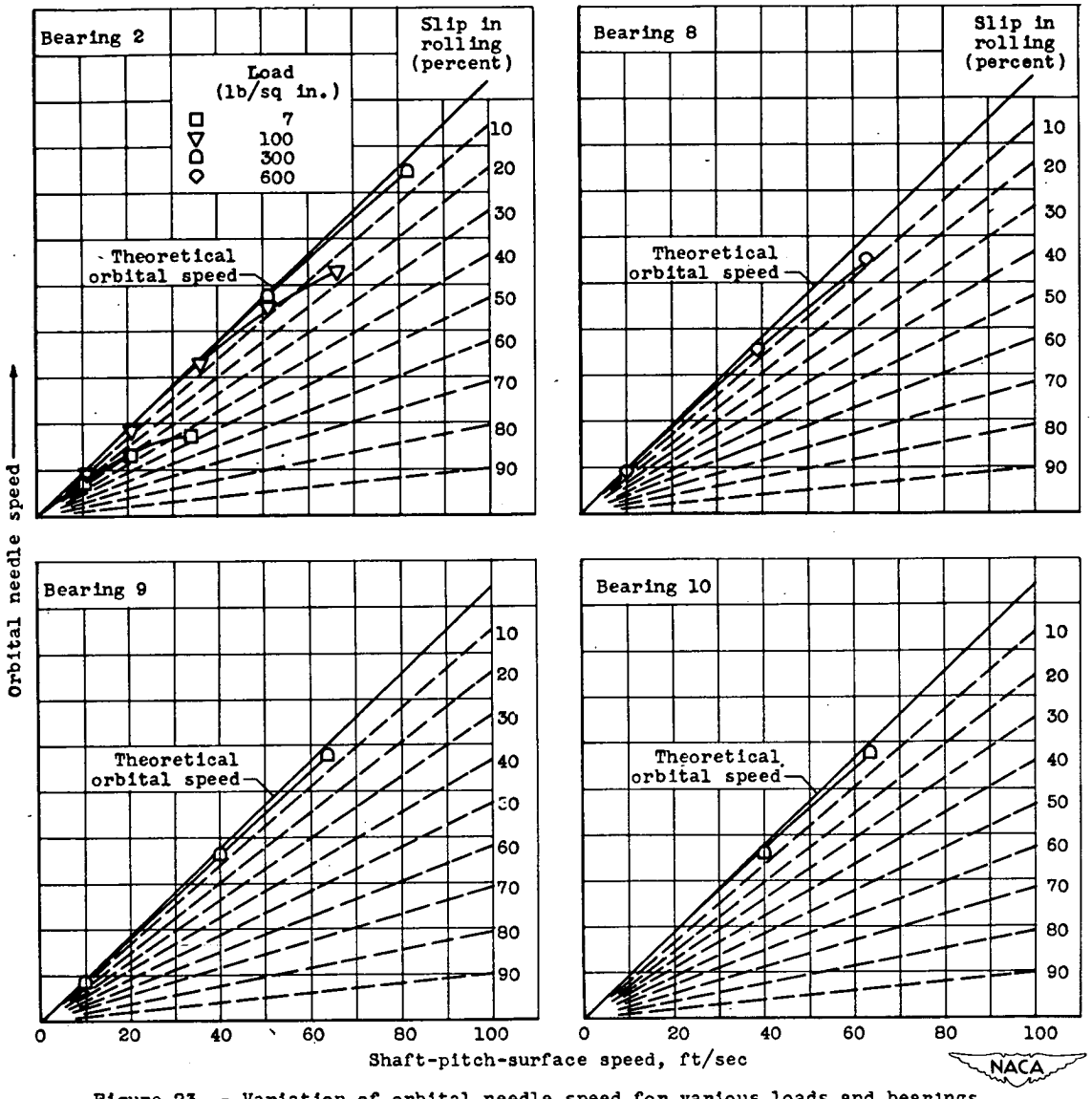

Figure 23. - Variation of orbital needle speed for various loads and bearings. (Stroboscopic light method.)

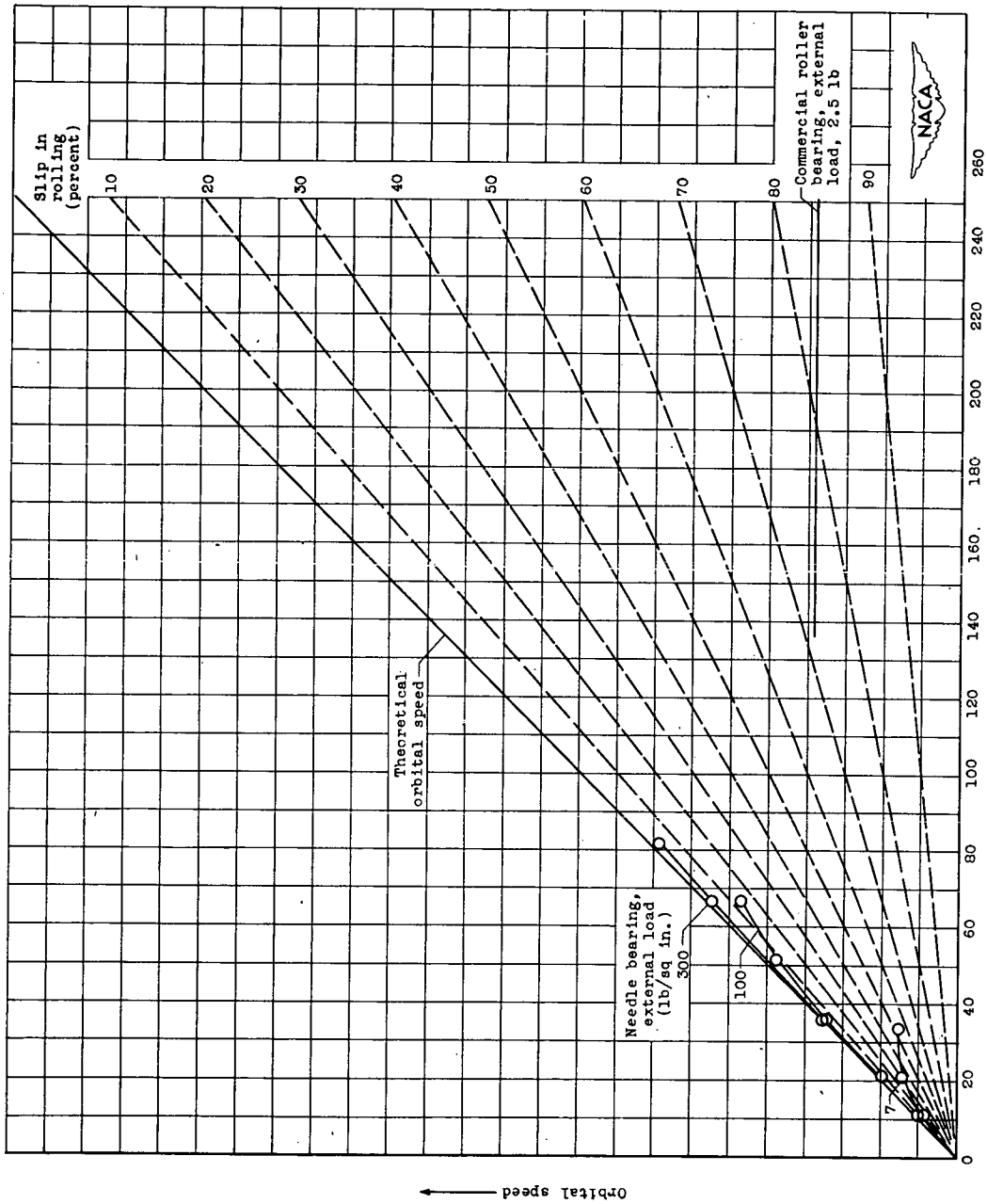

Figure 24. - Effect of shaft-pitch-surface speed on percentage of slip for needle bearing 3 (pitch diameter, 1.116 in.; effective length-diameter ratio of needles, 2.75; needle diameter, 0.1248 in.) and size 306 commercial roller bearing. Data for roller bearing taken from reference 16. (Stroboscopic light method for needle bearing.)

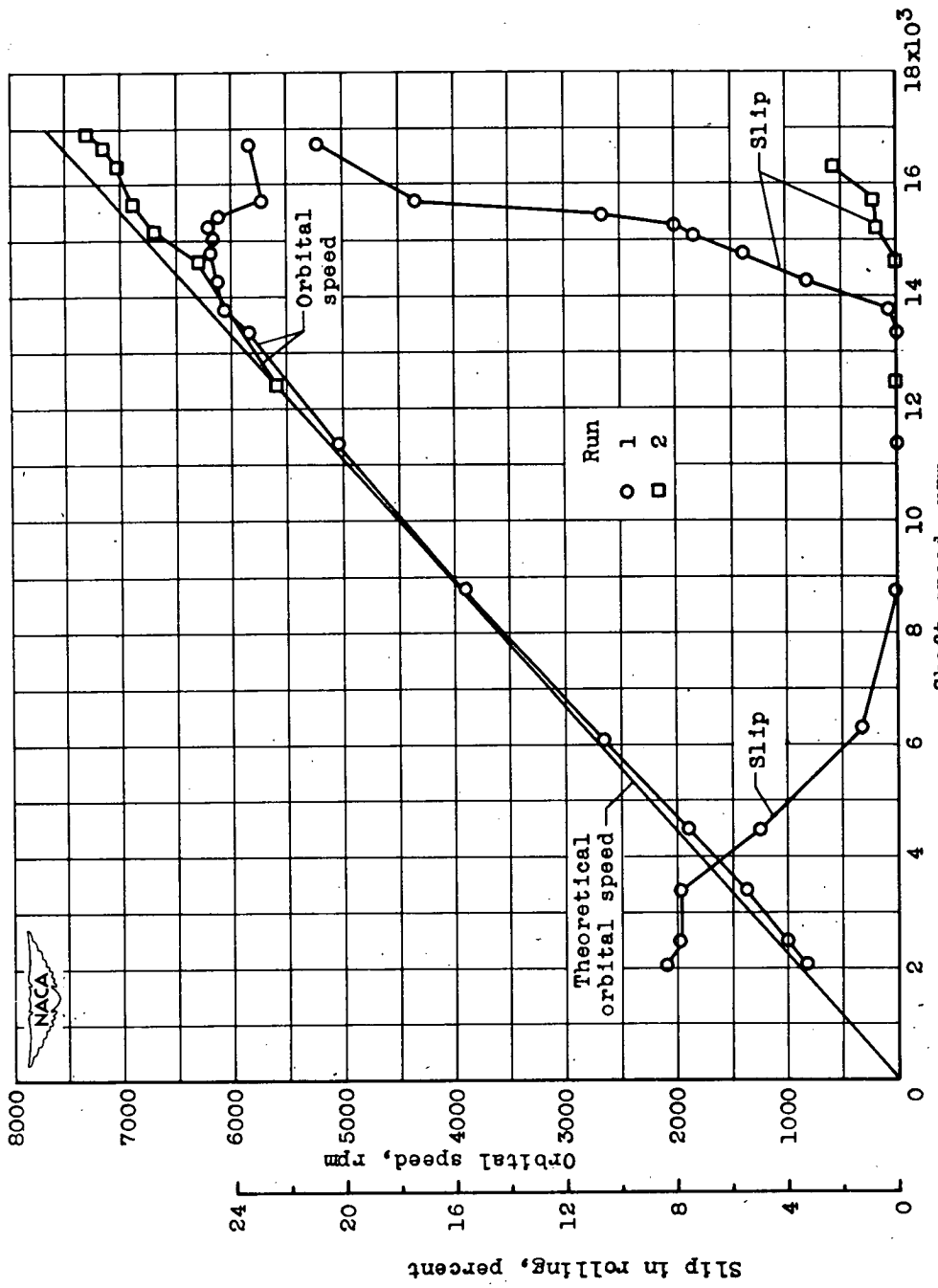

Figure 25. - Effect of shaft speed on percentage of slip and reproducibility of percentage of slip by magnetic pickup method for needle bearing 4. Pitch diameter, 1.116 inches; effective length-diameter ratio of needles, 2.75; needle diameter, 0.1249 inch; diametral clearance, 0.0025 inch; load, 7 pounds per square inch; oil flow, 2 pounds per hour.

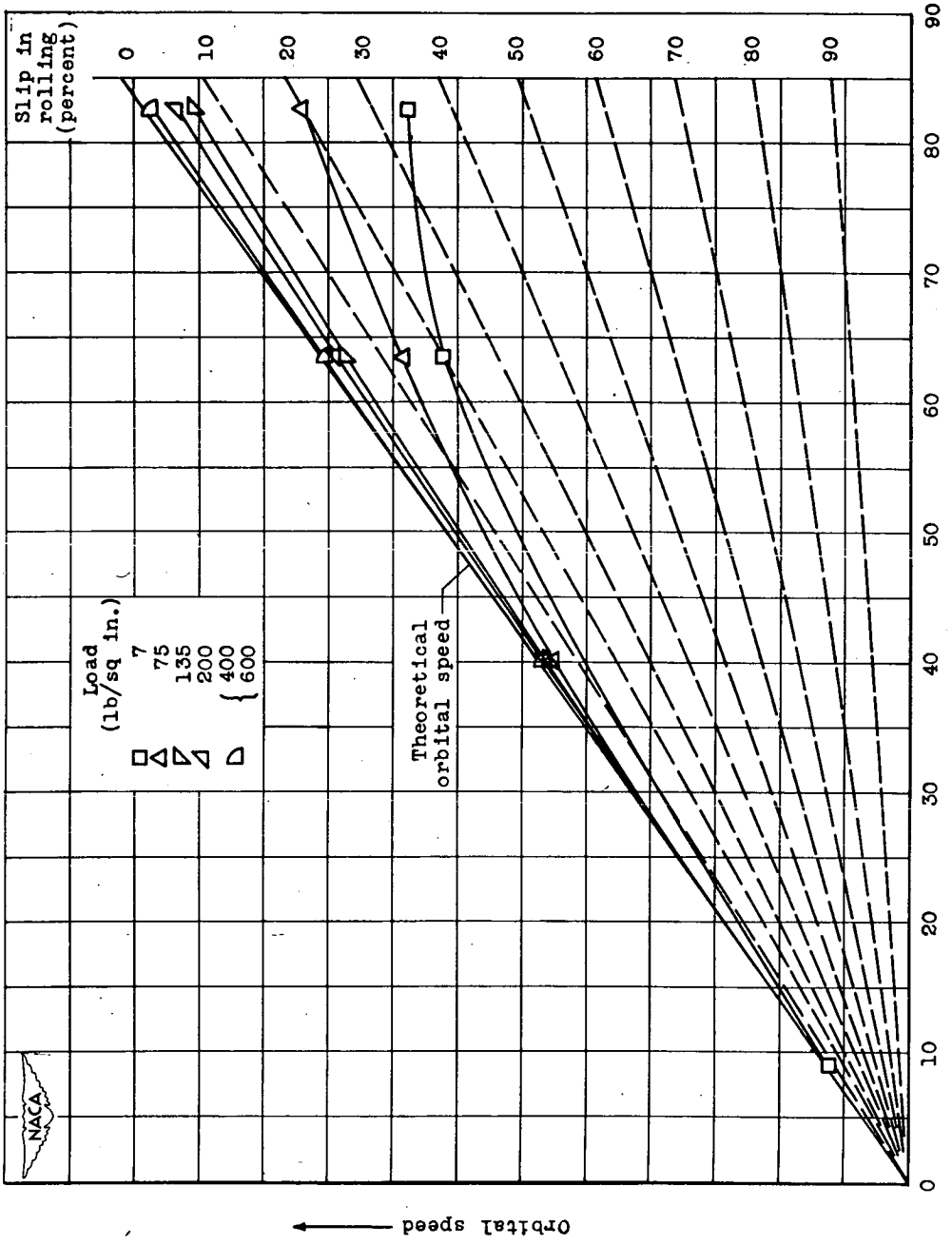

Figure 26. - Effect of shaft-pitch-surface speed on percentage of slip by magnetic pickup method for needle bearing 4. Pitch diameter, 1.116 inches; effective length-diameter ratio of needles, 2.75; needle diameter, 0.1249 inch; diametral clearance, 0.0025 inch; shaft speed, 2000 to 17,000 rpm; oil flow, 2 pounds per hour.

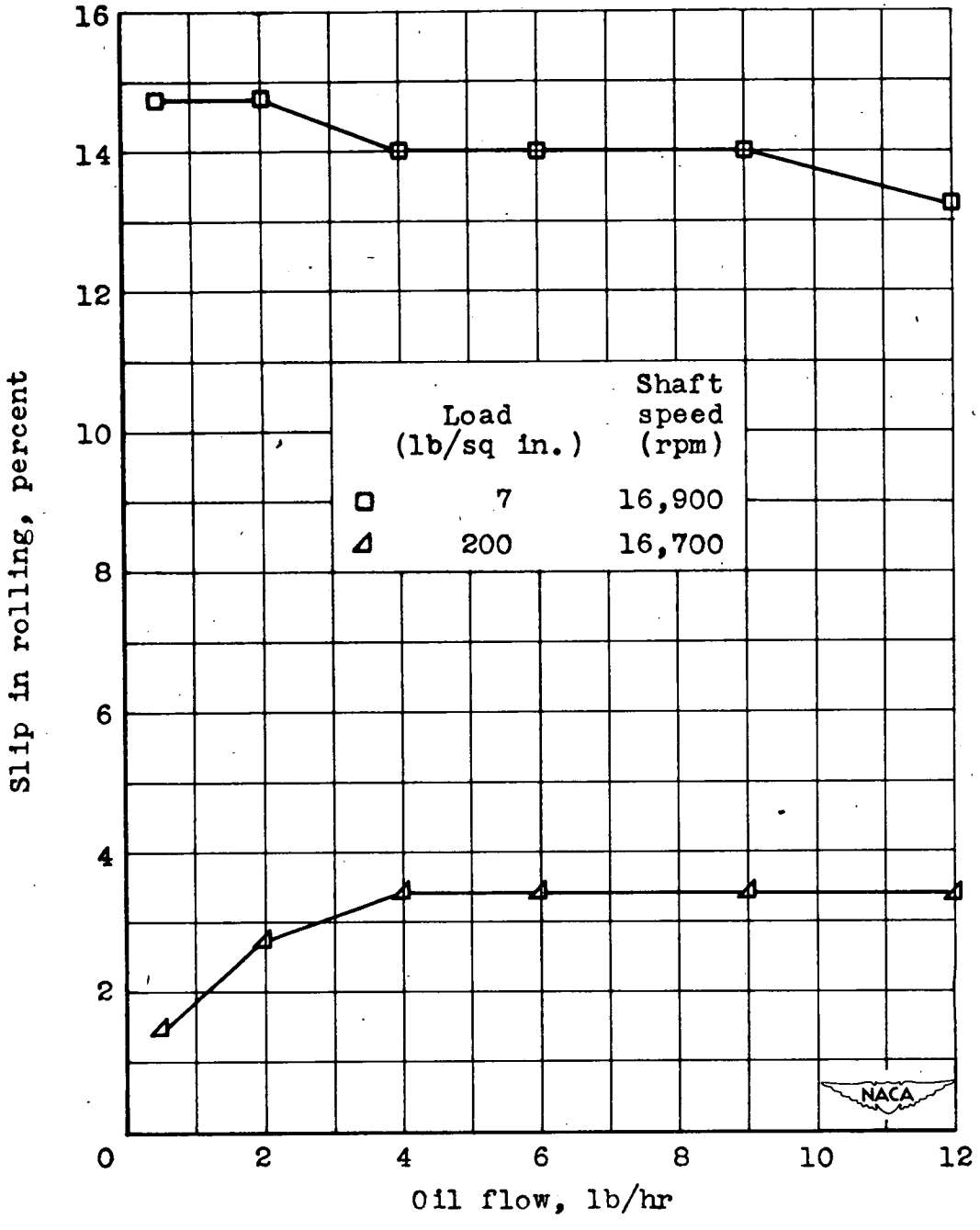

Figure 27. - Effect of oil flow on percentage of slip by magnetic pickup method of needle bearing 4. Pitch diameter, 1.116 inches; effective length-diameter ratio of needles, 2.75; needle diameter, 0.1249 inch; diametral clearance, 0.0025 inch.

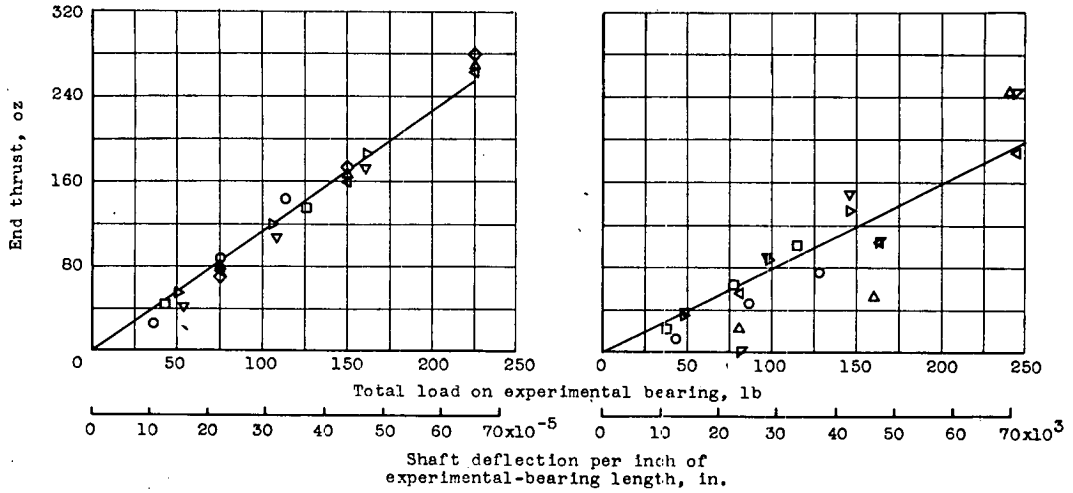

(a) Shaft speed, 2000 rpm.

(b) Shaft speed, 8000 rpm.

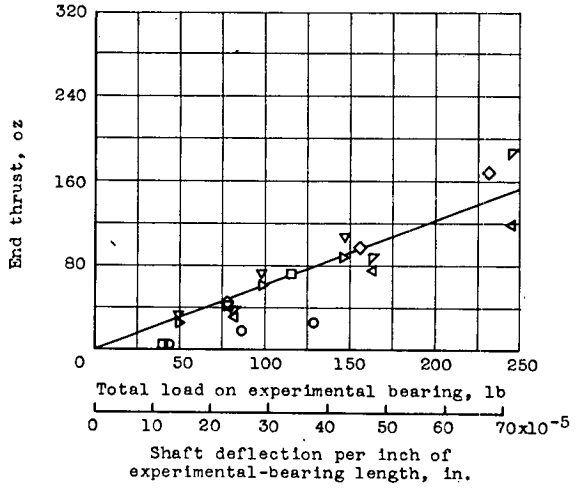

(c) Shaft speed, 13,000 rpm.

	Bearing	Pitch diameter (in.)	Effective length-diameter ratio	Needle diameter (in.)	Average diametral clearance (in.)	Number of needles
○	2	1.137	2.75	0.137	0.0010	26
□	3	1.116	2.75	.1249	.0018	28
◇	4	1.116	2.75	.1249	.0025	28
△	6	1.116	5.71	.1248	.0020	28
▽	7	1.117	3.50	.0625	.0016	56
▷	8	1.117	3.50	.0625	.0028	56
◁	9	1.117	11.67	.0624	.0017	56
▽	10	1.117	11.67	.0625	.0027	56

Figure 28. - Effect of load and shaft deflection on needle-bearing end thrust at shaft speeds of 2000, 8000, and 13,000 rpm.

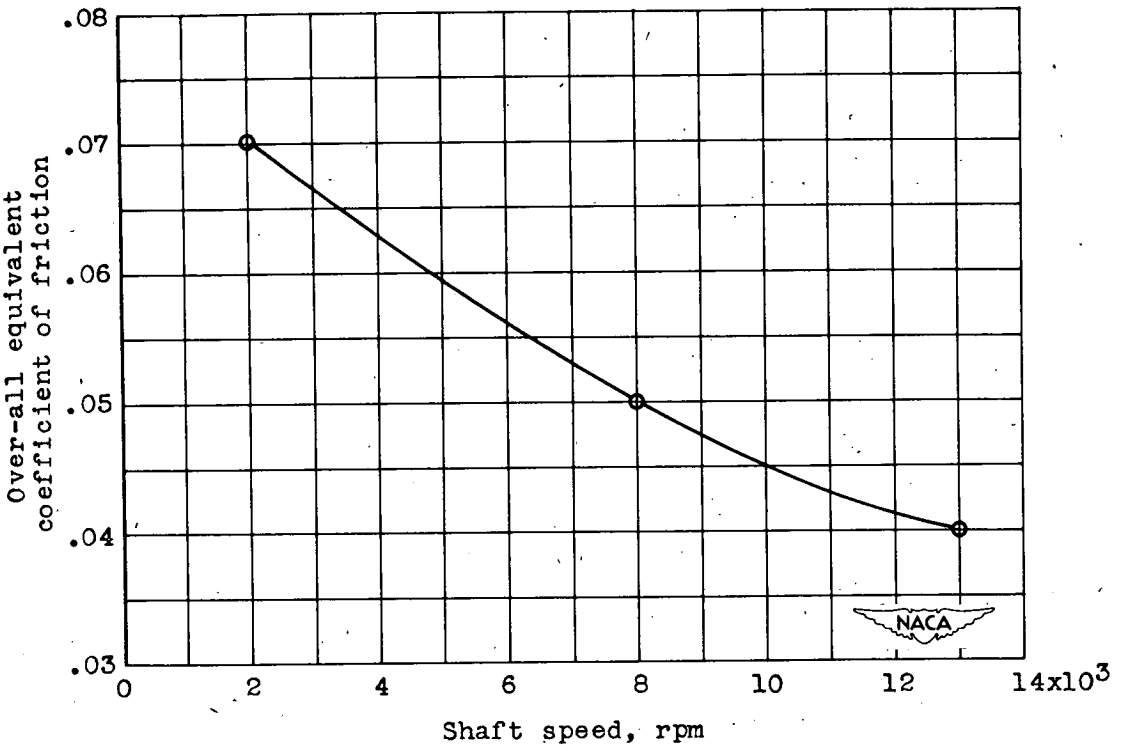

Figure 29. - Effect of shaft speed on over-all equivalent coefficient of friction of needle bearings.